Cosecant Square Pattern Synthesis With Conformal Antenna Arrays

Satish Kumar Reddy M V

Department of Electrical Engineering
National Institute of Technology,Rourkela
Rourkela-769008, Odisha, INDIA
May 2015

Cosecant Square Pattern Synthesis With Conformal Antenna Arrays

A thesis submitted in partial fulfilment of the
requirements for the degree of

Master of Technology

in

Electrical Engineering

by

Satish Kumar Reddy M V
(Roll-213EE1288)

Under the Guidance of

Prof.K. R. Subhashini

Department of Electrical Engineering
National Institute of Technology,Rourkela
Rourkela-769008, Odisha, INDIA
2013-2015

Department of Electrical Engineering

National Institute of Technology, Rourkela

C E R T I F I C A T E

This is to certify that the thesis entitled ***"Cosecant Square Pattern Synthesis With Conformal Antenna Arrays"*** *by* ***Mr. Satish Kumar Reddy M V****, submitted to the National Institute of Technology, Rourkela (Deemed University) for the award of Master of Technology in Electrical Engineering, is a record of bonafide research work carried out by him in the Department of Electrical Engineering , under my supervision. I believe that this thesis fulfils the requirements for the award of degree of Master of Technology.The results embodied in the thesis have not been submitted for the award of any other degree elsewhere.*

Prof.K. R. Subhashini

Place:Rourkela

Date:

To My Loving Family, Friends and Inspiring GUIDE

Acknowledgements

First and foremost, I am truly indebted to my supervisor Professor K. R. Subhashini for their inspiration, excellent guidance and unwavering confidence through my study, without which this thesis would not be in its present form. I also thank her for all the gracious encouragement throughout the work.

I express my gratitude to the members of Masters Scrutiny Committee, "Professors D. Patra, S. Das, P. K. Sahoo, Supratim Gupta" for their advise and care. I am also very much obliged to Head of the Department of Electrical Engineering, NIT Rourkela for providing all the possible facilities towards this work. I also thanks to other faculty members in the department for their invaluable support.

I would like to thank my colleagues "Pudu Atchutarao, Girijala Ravi Chandran, Chaudhari Manoj Govind ", for their enjoyable and helpful company I had with them.

My wholehearted gratitude to my parents, "M Jagannadha Reddy and M Thulasi" for their invaluable encouragement and support.

Satish Kumar Reddy M V

Rourkela, May 2015

Contents

Abstract

A modern high-speed aircraft will be installed with more than 25 antennas protruded from its structure for communication purpose, navigation, Instrumental Landing System etc. These multiple antennas can cause considerable amount of drag that will ultimately affect the efficiency of aircraft. Nowadays, integration of antennas on the surface of the aircraft is very much essential. So conformal arrays are well suitable for such applications. In this work, spherical, cylindrical and conical shaped antenna arrays have been modeled and discussed in detail. Further, these antenna arrays have been utilized to generate Cosecant-squared shaped radiation pattern that have importance in radar and navigation applications.

There is a significant difference in number of elements in linear and conformal array for the generation of cosecant squared radiation pattern. To bridge this gap, only certain elements, satisfying the constraints imposed on conformal antenna array are excited, and the cosecant squared radiation pattern is synthesised. The excitation parameters of the conformal array elements are optimized using DE & SSO optimization techniques.

Simulation results validate that radiation of cosecant squared shaped pattern is possible with the excitation of less number of elements for the different conformal array. Besides simulation results, the ripple value is calculated in the main lobe, and it is possible to get less ripple with the different constraint for the different conformal array.

List of Figures

List of Tables

List of Abbreviations

Abbreviation	Description
AF	Array Factor
DE	Differential Evolution
SSO	Simplified Swarm Optimization
PSO	Particle Swarm Optimization
lin	Linear
cir	Circular
sph	Spherical
cyl	Cylindrical
con	Conical
des	Desired
rand	Random
CSP	Cosecant square pattern
MLL	Main Lobe Level
SLL	Side Lobe Level

Chapter 1

Introduction

1.1 Introduction

According to the development in recent technology, every application goes wireless by transmitting and receiving electro magnetic signal through space. Antennas perform this transmission and reception of electro magnetic signals. As a single antenna element is unable to transmit or receive the required gain in the desired direction, systematic arrangement of individual antennas known as antenna array is used. Based on the alignment, antenna arrays are classified as 1D (linear array), 2D (circular array) and 3D-conformal arrays. The conformal array follows some prescribed shape and consists of antenna elements conforming to the surface. They are most preferred to reduce the aerodynamic drag for avionics applications. In this work, spherical, cylindrical and conical antenna arrays are modelled which are easily integrable with different structures. For air-surveillance radar sets, the Cosecant Square Pattern (CSP) is preferred, due to which a uniform signal strength is available at the receiver moving at a constant altitude. The synthesis of antenna arrays with analytical techniques like Taylor series method and Dolph Chebyshev methods is not efficient for shaped beam patterns like the flat-top pattern, cosecant squared pattern (CSP). The cosecant squared pattern can be treated as a nonlinear based optimization problem,for which the stochastic methods are necessary to synthesise. Differential Evolution (DE) and Simple Swarm

Optimization (SSO) techniques are employed to generate the desired cosecant square pattern.

1.2 Literature Review

The concept of antenna arrays [1] and detailed analysis of this field of work is very much important for the new research proposals in this area. Basic array formation[2], their characteristics and area of applications are required to have better understanding about antenna systems. Conformal arrays [3] has been studied in details.

Various optimization algorithms, their classification [4] and importance based on the requirements and desired constraints has been reviewed in details. Evolutionary algorithm "DE" [5, 6, 7] and nature-inspired optimization "SSO" [8, 9] that can be used efficiently in multi-objective function are referred in details along with their application methodology [10, 11].

The Cosecant-shaped beam formation [12] and their implementation with linear [13], circular [14] and spherical [15] arrays has been thoroughly studied and utilized in the present work.

The basics like design and development[16] of spherical antenna array, its element distributions as quasi uniform distribution and the Leopardi's algorithm distribution [17] are studied and the optimization of spherical antenna array[18] are utilised.

A complete analysis and design for conical array antenna for modern radar using a high resolution phase shifter[19] is studied. The microstrip conical antenna, the quadrifilar helix conical antenna[20] are studied for GPS application.

The array factor formulations of cylindrical array and optimization of excitation parameters [21] is studied. Design of a Cylindrical Polarimetric Phased Array Radar Antenna [22] is studied for Weather Sensing Applications

1.3 Objectives

The primary objectives of the thesis are mentioned as below:

- Design and synthesis of spherical, cylindrical and conical antenna arrays using the concepts of basic antenna arrays (Linear & Circular).
- Optimization of complex excitation parameters by using evolutionary algorithm DE and nature-inspired algorithm SSO for the generation of cosecant squared pattern.
- Simulation-based study of the performance of elements on an azimuthal plane of the conformal array for the generation of CSP.
- To achieve threshold ripple value in main lobe of desired cosecant square pattern.

1.4 Thesis Organization

The thesis is organised as follows.

- Chapter 2 gives a brief introduction of linear and circular antenna arrays. Further, the design of spherical, cylindrical and conical antenna arrays deploying two primary conventional arrays have been discussed.
- Chapter 3 discusses the applications of Cosecant Squared Pattern and introduction of DE and SSO algorithms. Beside that Synthesis of the cosecant squared pattern has been carried out with the aid of DE & SSO on spherical, cylindrical and conical antenna arrays.
- Chapter 4 introduces the detriment of the conformal array over the linear array for the synthesis of cosecant square pattern and a method to overcome that. This method has been applied for the spherical, cylindrical and conical arrays to synthesize the cosecant squared pattern.
- Chapter 5 concludes the entire research work carried out and gives an insight to the future scope.

Chapter 2

Antenna Arrays

Achieving a high directive gain and lower sidelobe level may not be possible with single antenna element in many applications. In such instances, there are two primary techniques to enhance the performance of antenna systems. One of the methods is to vary the dimensions of the single antenna elements which is impractical in many applications. The other method is to form an antenna array that is a systematic arrangement of the individual antenna elements. The amount of radiated field from an antenna array at a point of space is calculated as the vector sum of the radiated field by every single element at that point[1]. Thus the total field of an array at a reference point is related to field of a single element as below:

$$E_{total} = [E_{single\ element}] * [Array\ Factor]$$

Where, Array Factor is a function dependent on geometrical parameters as shape, spacing between elements and electrical parameters as amplitude and phase of current excitations for the elements.

2.1 Linear Array

A linear array is a one-dimensional array, which is an arrangement of usually identical elements in a straight line. A linear array of M isotropic element placed along Z axis having a uniform space of d between the elements is as

shown in fig.2.1. and the array factor[1] is given as:

$$AF_{lin}(\theta,\phi) = \sum_{m=1}^{M} I_m * exp^{j[(m-1)kd\cos\theta+\beta]} \tag{2.1}$$

where, β is the progressive phase shift between adjacent elements

$k$is the propagation constant

I_m is the complex excitation of m^{th} element.

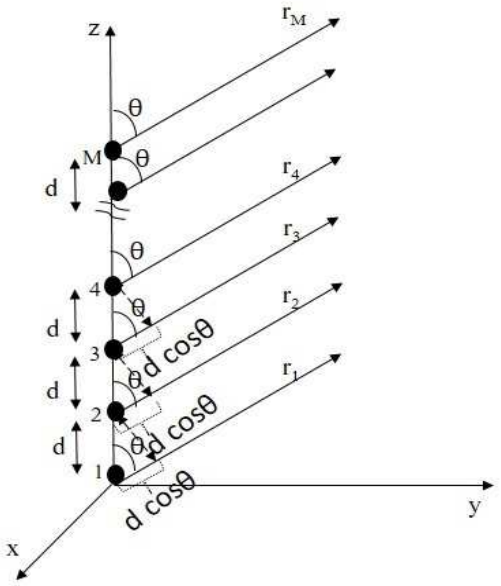

Figure 2.1: Linear Antenna Array

2.2 Circular Array

A circular array is a two-dimensional array, which is an alignment of usually identical elements along the circumference of a circle. A circular array of N isotropic elements with uniform inter-element spacing is placed in XY plane with centre at its origin is as shown in fig.2.2. The array factor for this circular array is given as:

$$AF_{cir}(\theta,\phi) = \sum_{n=1}^{N} I_n * exp^{j[ka\sin\theta\cos(\phi-\phi_n)+\alpha_n]} \tag{2.2}$$

where, ϕ_n is the angular position of n^{th} element on the circle

I_n is the excitation amplitude of n^{th} element

α_n is the excitation phase of n^{th} element

a is the radius of the circle.

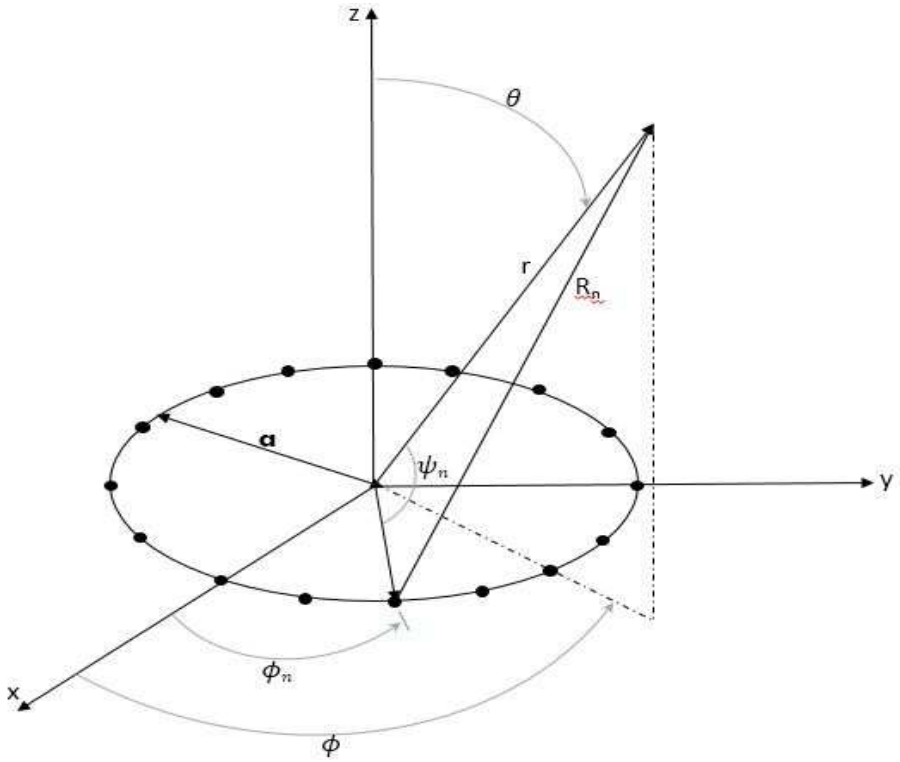

Figure 2.2: Circular Antenna Array

2.3 Conformal Arrays

The conformal arrays are three dimensional array that has radiating elements following some prescribed shape. A conformal array is designed to integrate on the curved surfaces for reduction of aerodynamic drag.

2.3.1 Spherical Array

The spherical antenna array is one of the conformal array of huge interest. An adorable feature of the spherical antenna array is that, as its elements are symmetrically aligned, the radiation pattern at any far field point over the space will view the analogous environment. The spherical antenna array can

be operated to achieve multiple beam and shaped radiation patterns based on signal processing and electronic beam steering capabilities.[3].

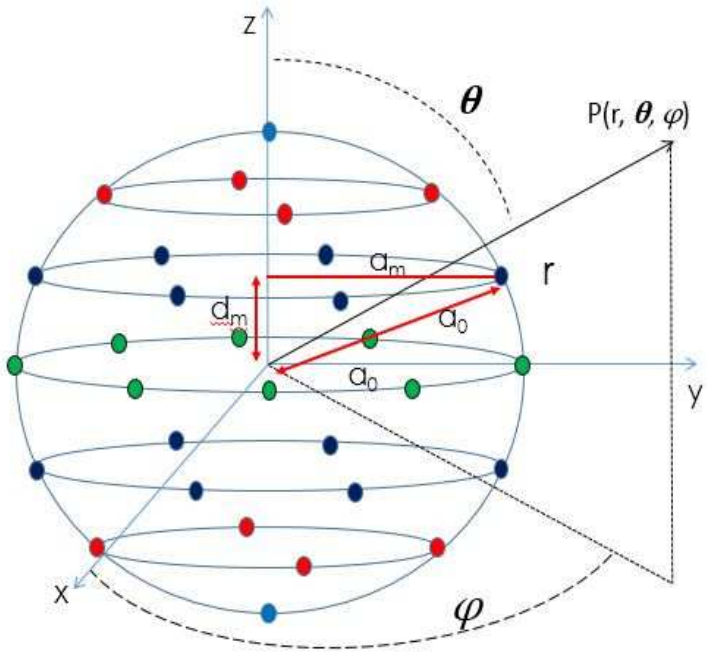

Figure 2.3: Spherical Antenna Array

Array Factor Formulation of Spherical Array

The spherical antenna array can be modelled as arrangement of circular arrays one over the other. The radius of the circular arrays follows a definite set of rules and decreases as we progress away from the centre of sphere.The arrangement of spherical array is as shown in fig. 2.3.In this work a spherical array is designed by alignment of $2M + 1$ circular arrays of different radius a_m and each circular array consists of N_m discrete and identical elements. As the radius varies and to have the equal inter element spacing of the circular array, the number of elements N_m varies for different circular array.The array factor for m^{th} circular array of spherical array can be rewritten from equation 2.2 as:

$$AF(\theta, \phi) = \sum_{n=1}^{N} I_n exp^{(jka_m \sin(\theta) \cos(\phi - \phi_n) + j\psi_n)} \tag{2.3}$$

where, a_m is radius for m^{th} circular array can be calculated and given as in fig. 2.2

$$a_m = sqrt(a_0^2 - d_m^2)$$

To form a spherical geometry, such circular arrays are to be arranged in a linear fashion.The linear array factor for 2M+1 antenna elements can be rewritten from equation 2.1 as:

$$AF_{lin}(\theta, \phi) = \sum_{m=-M}^{M} I_m * exp^{j[nkd_m \cos\theta + \beta]} \tag{2.4}$$

Hence, a spherical antenna array modelled with $2M+1$ circular array stacks can be represented by combining equations 2.4& 2.3 as:

$$AF_{sph}(\theta, \phi) = \sum_{n=1}^{N_m} I_n exp^{(jka_m \sin(\theta)\cos(\phi - \phi_n) + j\psi_n)} * \sum_{m=-M}^{M} I_m * exp^{j[mkd_m \cos\theta + \beta]} \tag{2.5}$$

Rearranging the above equation, we have

$$AF_{sph}(\theta, \phi) = \sum_{m=-M}^{M} \sum_{n=1}^{N_m} I_{nm} exp^{(jka_m sin(\theta) cos(\phi - \phi_{nm}) + j\psi_n) + (jkd_m cos(\theta) + \beta_m)} \tag{2.6}$$

The above defined array factor expression gives a truncated spherical array with a slice at its top and bottom surface. Hence, to form a complete spherical array, an antenna element is added both at its top and bottom surface.The final expression for the spherical array factor with $2M+1$ circular array can be re-written as:

$$AF_{sph}(\theta, \phi) = \sum_{m=-M}^{M} \sum_{n=1}^{N_m} I_{nm} exp^{(jka_m sin(\theta) cos(\phi - \phi_{nm}) + j\psi_n) + (jkd_m cos(\theta) + \beta_m)} + exp^{(jka_0 \cos\theta)} + exp^{(-jka_0 \cos\theta)} \tag{2.7}$$

where,

I_{nm} is the current excitation for n^{th} antenna element of m^{th} circular array,

k is the propagation constant,

θ is the elevation angle,

ϕ is the azimuth angle,
ϕ_{nm} is the azimuth position of n^{th} antenna element on m^{th} circular array,
a_m is the radius for m^{th} circle of spherical array and is given as in fig. **??**:

$$a_m = sqrt(a_0^2 - d_m^2)$$

a_0 is the radius of spherical array,
ψ_n is the beam steering phase angle in azimuth direction,
d_m is the distance of m^{th} circular array from reference circular array at the origin,
β_m is the progressive phase shift between m^{th} and reference circular array.

2.3.2 Cylindrical Array

An attractive feature of cylindrical array is that, any point in far-field the beam is formed at the bisector of the cylindrical sector, and the cross-polarizations caused by opposing elements in azimuth cancel each other. A Cylindrical antenna array can be observed as a linear assembly of circular array mounted one above the other such that the radius of all circular arrays is constant as shown in Fig.2.4 . Hence, the basic foundation of cylindrical array is taken from field equations of a circular array and linear array.

Array Factor Formulation of Cylindrical Array

For modelling cylindrical shaped array, the geometry can be viewed as it(cylindrical array) is a linear stack arrangement of circular antenna array placed one above the other such that the radius of all stacked circular arrays is constant as given in fig. 2.4. Here, cylindrical array is modelled by taking $2M + 1$ circular array of equal radius r in stack with each circular array consist of N discrete and similar set of antenna elements. The array factor for m^{th} circular array of cylindrical array can be rewritten from equ. 2.8 as:

$$AF_{cir}(\theta, \phi) = \sum_{n=1}^{N} I_n exp^{(jkr \sin(\theta) \cos(\phi - \phi_n) + j\psi_n)} \tag{2.8}$$

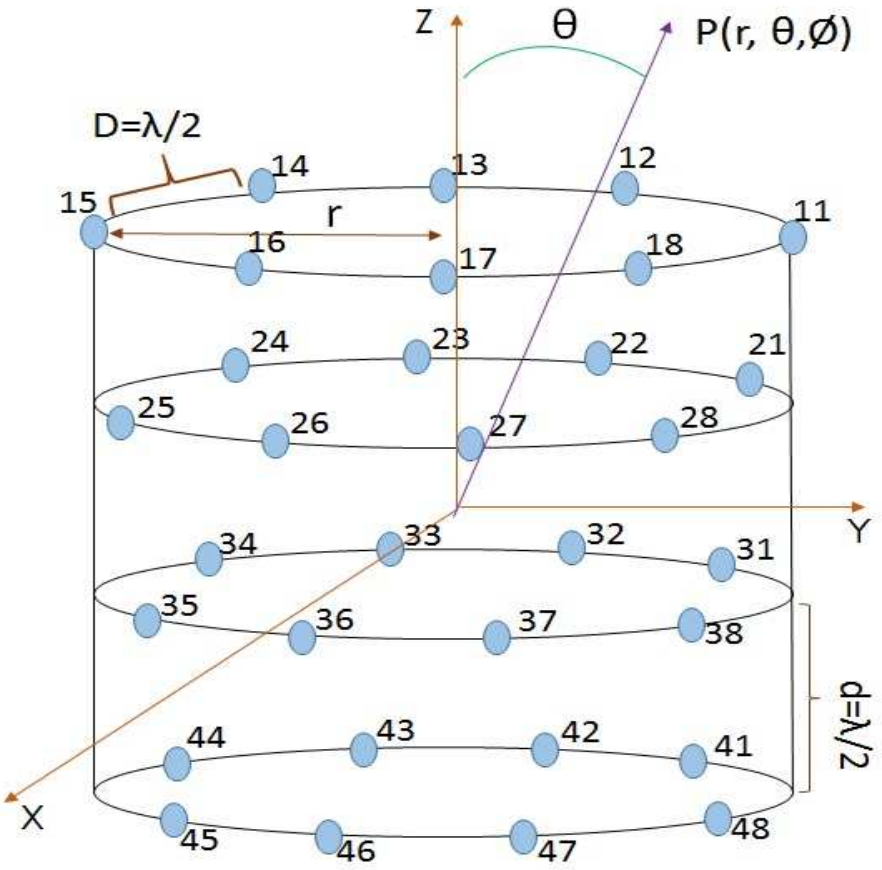

Figure 2.4: Cylindrical Antenna Array

where, r is radius for m^{th} circular array can be calculated and given as in fig. 2.4 $r = \frac{D*N}{2pi}$ To form a cylindrical geometry, such circular arrays are to be arranged in a linear fashion.The linear array factor for $2M+1$ antenna elements can be rewritten from equ. 2.9 as:

$$AF_{lin}(\theta,\phi) = \sum_{m=-M}^{M} I_m * exp^{j[kd_m \cos\theta+\beta]} \tag{2.9}$$

Hence, a cylindrical antenna array modelled with $2M+1$ circular array stacks can be represented by combining 2.8 & 2.9 as:

$$AF_{cyl}(\theta,\phi) = \sum_{n=1}^{N} I_n exp^{(jkr\sin(\theta)\cos(\phi-\phi_n)+j\psi_n)} * \sum_{m=-M}^{M} I_m * exp^{j[kd_m\cos\theta+\beta_m]} \tag{2.10}$$

Rearranging the above equation, we have

$$AF_{cyl}(\theta,\phi) = \sum_{m=-M}^{M}\sum_{n=1}^{N} I_{nm} exp^{(jkrsin(\theta)cos(\phi-\phi_{nm})+j\psi_m)+(jkd_m cos(\theta)+\beta_m)} \quad (2.11)$$

where,
I_{nm} is the current excitation for n^{th} antenna element of m^{th} circular array,
k is the propagation constant,
θ is the elevation angle,
ϕ is the azimuth angle,
ϕ_{nm} is the azimuth position of n^{th} antenna element on m^{th} circular array,
r is the radius of circle of cylindrical array and is given as in fig. 2.4: $r = \frac{D*N}{2pi}$
ψ_m is the beam steering phase angle in azimuth direction,
d_m is the distance of m^{th} circular array from reference circular array at the origin,
β_m is the progressive phase shift between m^{th} and reference circular array.

2.3.3 Conical Array

The cone array geometry, chosen for its similarity to an aircraft or missile nose cone, is considered for several important performance parameters including scan volume, side lobe control. A conical antenna array can be observed as a linear assembly of circular array mounted one above the other such that the radius of each circular array follow the property of cone as shown in Fig.2.5. Hence, the Array factor formulation of conical array is derived from the array factor of circular array and linear array.

Array Factor Formulation of Conical Array

For modelling conical shaped array, the geometry can be viewed as it(conical array) is a linear stack arrangement of circular antenna array placed one above the other such that, the radius of each progressive stacked circular

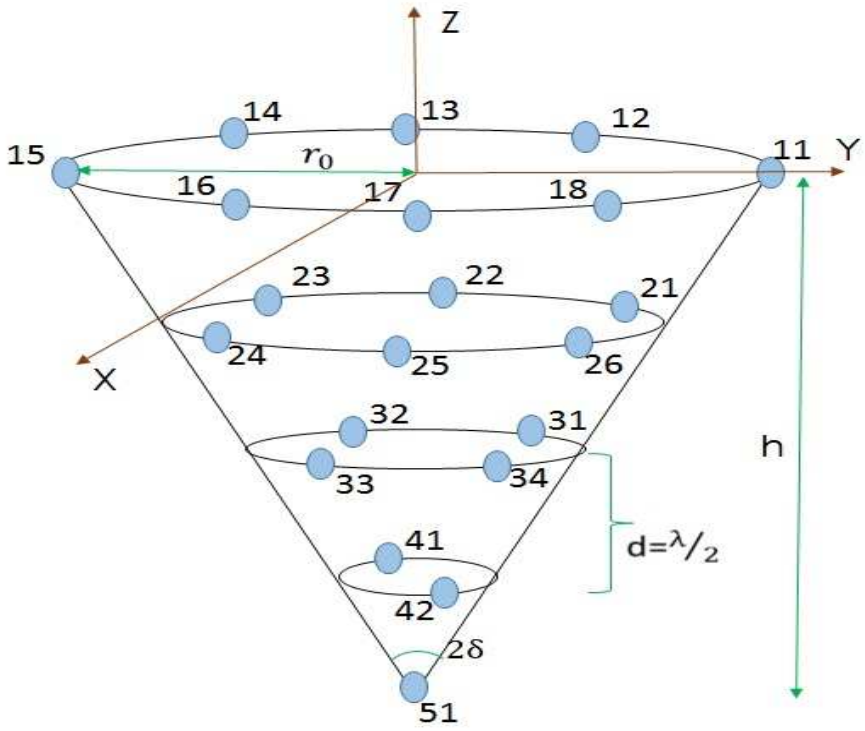

Figure 2.5: Conical Antenna Array

array follow a definite set of rules to form a conical shaped array as given in fig. 2.5. Here, conical array is modelled by taking M circular array of varying radius r_m in stack with each circular array consist of N discrete and similar set of antenna elements. The array factor for m^{th} circular array of spherical array can be rewritten from equ. 2.12 as:

$$AF(\theta,\phi) = \sum_{n=1}^{N} I_n exp^{(jkr_m \sin(\theta)\cos(\phi-\phi_n)+j\psi_n)} \tag{2.12}$$

where, r_m is radius for m^{th} circular array can be calculated and given as in fig. 2.5 $r_m = \tan\delta * d_m$ To form a conical geometry, such circular arrays are to be arranged in a linear fashion.The linear array factor for M antenna elements can be rewritten from equ. 2.13 as:

$$AF_{lin}(\theta,\phi) = \sum_{m=1}^{M} I_m * exp^{j[kd_m \cos\theta+\beta]} \tag{2.13}$$

Hence, a spherical antenna array modelled with M circular array stacks can be represented by combining 2.12 & 2.13 as:

$$AF_{con}(\theta,\phi) = \sum_{n=1}^{N_m} I_n exp^{(jkr_m \sin(\theta)\cos(\phi-\phi_n)+j\psi_n)} * \sum_{m=1}^{M} I_m * exp^{j[kd_m\cos\theta+\beta]} \quad (2.14)$$

Rearranging the above equation, we have

$$AF_{con}(\theta,\phi) = \sum_{m=1}^{M}\sum_{n=1}^{N_m} I_{nm} exp^{(jkr_m sin(\theta)cos(\phi-\phi_{nm})+j\psi_n)+(jkd_m cos(\theta)+\beta_m)} \quad (2.15)$$

The above defined array factor expression gives a truncated conical array with a slice at its vertex. Hence, to form a complete conical array, an antenna element is added vertex. The final expression for the conical array factor with M circular array can be re-written as:

$$AF_{con}(\theta,\phi) = \sum_{m=1}^{M}\sum_{n=1}^{N_m} I_{nm} exp^{(jkr_m sin(\theta)cos(\phi-\phi_{nm})+j\psi_n)+(jkd_m cos(\theta)+\beta_m)} + exp^{(-jkh\cos\theta)} \quad (2.16)$$

where,

I_{nm} is the current excitation for n^{th} antenna element of m^{th} circular array,

k is the propagation constant,

θ is the elevation angle,

ϕ is the azimuth angle,

ϕ_{nm} is the azimuth position of n^{th} antenna element on m^{th} circular array,

r_m is the radius for m^{th} circle of spherical array and is given as in fig. 2.5:

$r_m = \tan\delta * d_m$

δ is the angle of conical array,

ψ_m is the beam steering phase angle in azimuth direction,

d_m is the distance of m^{th} circular array from origin,

β_m is the progressive phase shift between m^{th} and reference circular array.

Chapter 3

Cosecant Square Pattern

In modern technology, shaped-beams are widely used in satellite and radar based applications. Cosecant-square pattern(CSP) is one such pattern which is generally employed for long-range systems requiring higher gain near the horizon with low gain at higher elevation angles. During detection of an aircraft flying in space, it will be observed at a closer range at higher elevation angles, so use of such pattern significantly limits the power available to aircraft at higher elevation angles thereby providing a uniform signal strength to the aircraft throughout its journey. Thus, the cosecant squared pattern distribution [12] as shown in fig. 3.1 is a means of achieving a uniform signal strength at the input of the receiver of target when it is moving at a constant altitude.

3.1 Mathematical Justification of Cosecant-Squared Pattern

Consider an aircraft is flying at a constant height 'H' in an Air Surveillance radar System as shown in fig. **??**. As it can be clearly observed that as the aircraft is moving towards the radar system, its range 'R' keeps on decreasing with an increase in its elevation angle 'ε'. Thus, due to this continuous variation in the range of aircraft, the echo power received by radar receiver keeps on changing. Thus, in order to receive uniform echo power by the receiver, the radiation shape needs to be modified to Cosecant-square shape. It can

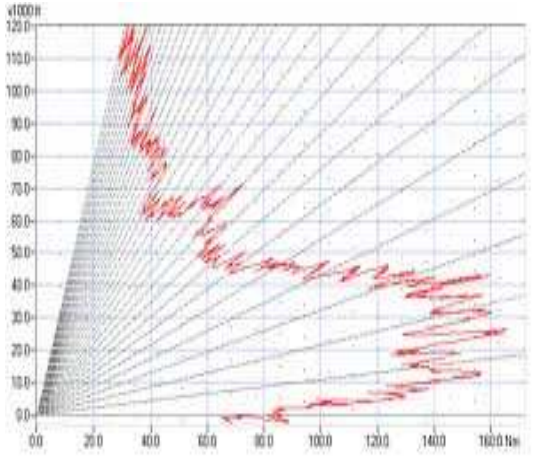

(a) A Practical Cosecant-Squared pattern Reference:radartutorial.eu

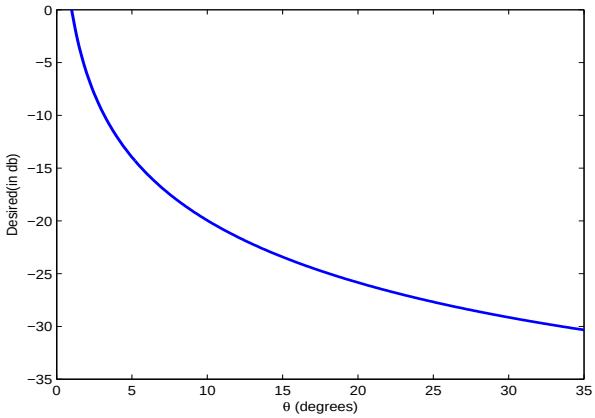

(b) Simulated Cosecant-Squared pattern

Figure 3.1: Cosecant Square Radiation Pattern

be justified from the derivation as below:

The height H and the range R define the elevation angle ... By trigonometric relation, we have

$$R = \frac{H}{sin(\varepsilon)} \Rightarrow R = Hcosec(\varepsilon) \tag{3.1}$$

If the echo has a uniform signal strength at the input of the receiver than

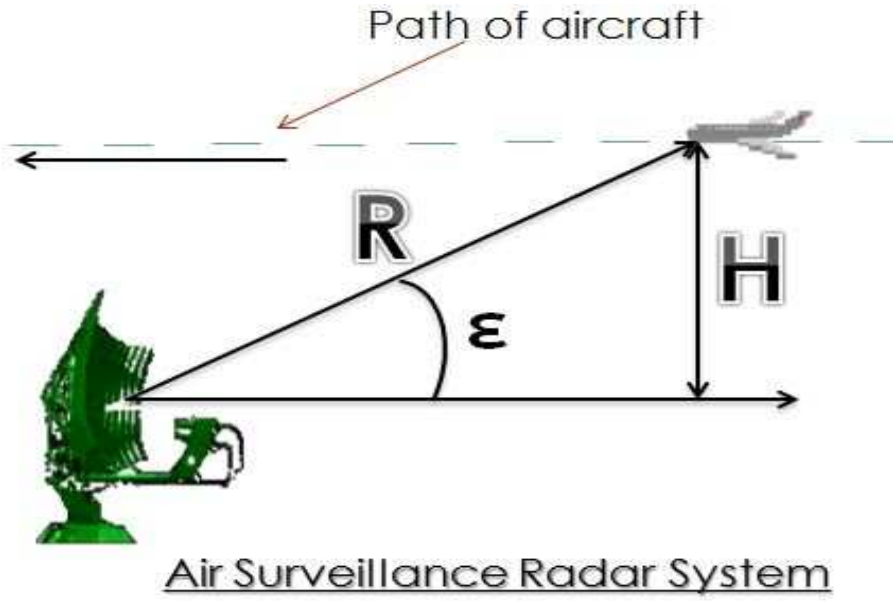

Figure 3.2: Air surveillance Radar System

the range is dependent on the square of the antenna gain in the fourth power linearly.

$$P_r \sim \frac{G^2}{R^4} \tag{3.2}$$

To receive uniform power by the aircraft P_r=constant Using above condition, we have

$$G^2 \sim R^4 \tag{3.3}$$

which will be further reduced to,

$$G \sim R^2 \tag{3.4}$$

Now using equation (3.1) in equ (3.4) we get,

$$G = (cosec(\varepsilon))^2 \tag{3.5}$$

3.2 Optimization Algorithms

The above discussed cosecant-squared pattern is one specific pattern and has to be generated with various antenna arrays. To generate this pattern, we requires some definite combination of radiation pattern controlling parameters for array like excitation amplitude, phase, inter-element spacing etc so that the newly generated radiation pattern tends to approximate the desired radiation pattern. In present scenario, it is observed that many such problem statement requires efficient use of optimization algorithms [4] to reach the desired solutions under various constraints. Nowadays, stochastic-based optimization algorithms has become ineffective in several research areas. Due to this, Evolutionary algorithms and Swarm-based optimization due to their global behaviour and less number of controlling parameters are getting more importance. Here, DE and SSO algorithms are discussed in details and are applied to achieve the objective of this thesis.

3.2.1 Differential Evolution Algorithm

Differential Evolution(DE) algorithm, proposed by Price and Storn in 1996, is a stochastic population-based evolutionary algorithm [5] for optimizing multi-dimensional space variables. In present scenario, there are so many problems whose objective function are non-linear, noisy, flat and multi-dimensional having more than one local minima and other constraints. Such problems are difficult to solve analytically, hence DE based technique can be well utilized to find an approximate result for such problems [10]. Moreover, compared to other algorithms DE is more simpler and straightforward to implement with very few control parameters (F, CR and N). It is extremely capable in providing multiple solutions in a single run with lower value of space complexity. However, the convergence rate of DE algorithm is quite higher in comparison to other class of algorithms [5]. This class of evolutionary algorithms follows four basic steps [7, 6] as Initialization, Mutation, Recombination and Selection for its operation.

1. Initialization: To optimize a function with D real parameters, we have to select a population of size N (at least of size 4)with the parameter vector 'x' given as:

$$x_i, G = [x_{1,i,G}, x_{2,i,G}, \ \ldots\ldots\ x_{D,i,G}]$$

where, i = 1, 2, . . . , N

G is the generation number

The vector x is selected randomly from its bounded range $[x_j^L, x_j^U]$.

where, x_j^L is lower limit,

x_j^U is upper limit

After initialisation of every vector of the population, its corresponding fitness value is computed and best of these is stored for future reference.

2. Mutation: Now for each given parameter $x_{i,G}$, we will select three random vectors $x_{r1,G}$,$x_{r2,G}$ and $x_{r3,G}$ with distinct indices i, r_1, r_2 and r_3. Apply

mutation on it using equation as below:

$$v_{i,G+1} = x_{r1,G} + F(x_{r2,G} \sim x_{r3,G})$$

where, F is the mutation factor, such that F∈[0,2]

$v_{i,G+1}$ is called as donar vector

3. Recombination: Now recombination uses successful solutions obtained from the previous generation and generates a new trial vector from the elements of the previous target vector $x_{i,G}$ and the elements of the newly created donar vector $v_{i,G+1}$ based on the following relation:

$$u_{j,i,G+1} = \begin{cases} v_{j,i,G+1}, & \text{if } rand_{j,i} \leq \text{CR or } j = I_{rand} \\ x_{j,i,G}, & \text{if } rand_{j,i} > \text{CR and } j \neq I_{rand} \end{cases}$$

where,i = 1, 2, . . . , N ;

j = 1, 2, . . . , D

I_{rand} is a random integer[1,2,.....D] such that, $v_{i,G+1} \neq x_{j,i,G}$

4. Selection: Finally, selection for next generation vector is done by comparing fitness value due to trial vector $v_{i,G+1}$ and target vector $x_{i,G}$ using criteria

$$x_{i,G+1} = \begin{cases} x_{i,G+1}, & \text{if } f(u_{1,G+1}) \leq f(x_{1,G}) \\ x_{i,G}, & \text{otherwise} \end{cases}$$

Now, the process of Mutation, Recombination and Selection is repeated till some stopping criterion as defined in the algorithm is reached.

The concept of DE algorithm process is presented with the flowchart [11] shown by fig. 3.3 as:

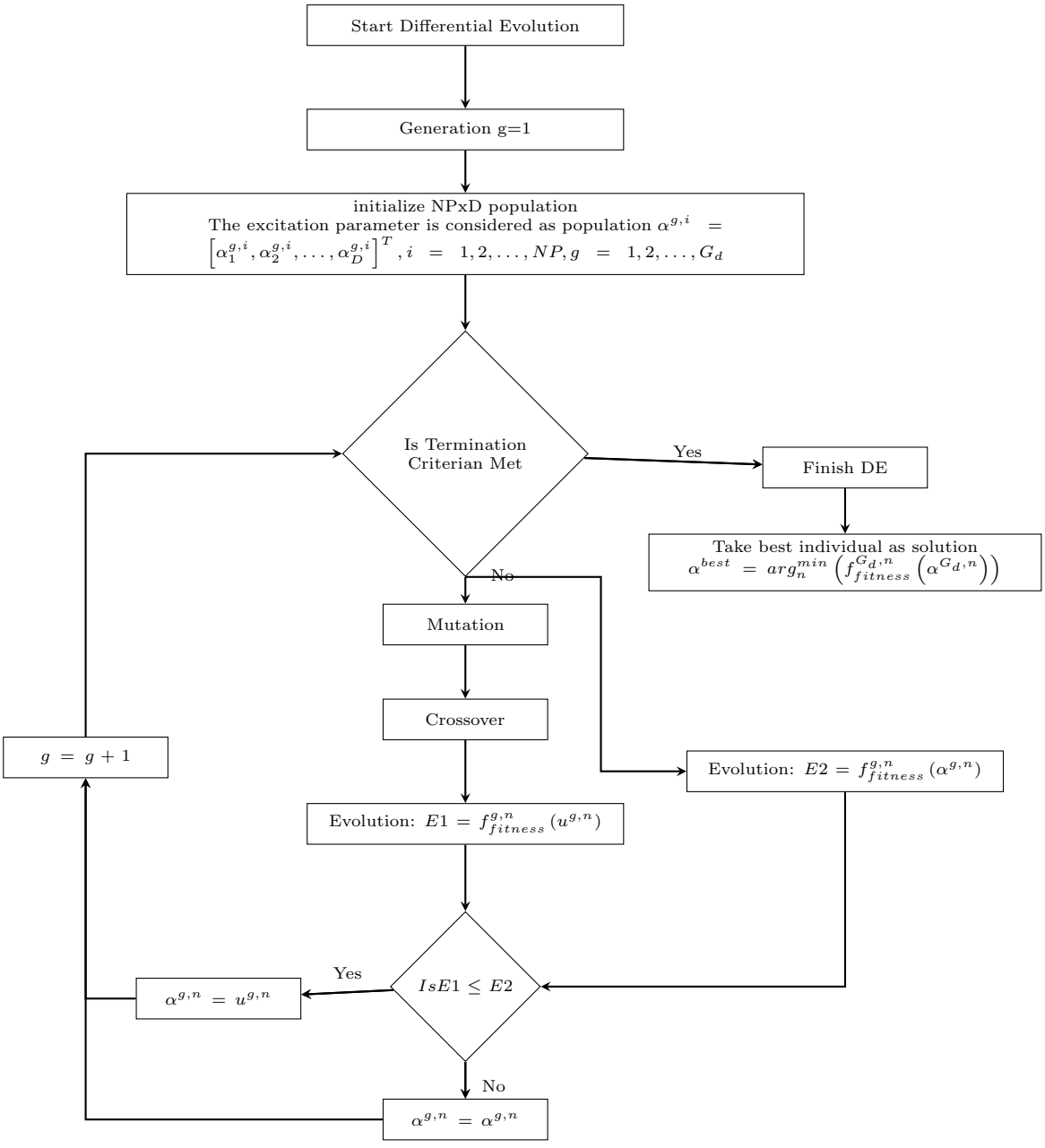

Figure 3.3: Flowchart of Differential Evolution Algorithm

Validation of DE with the Published Work

Referred to [23] of Symmetric Linear array with 24 elements with uniform spacing of 0.5λ to minimise the SLL value. It is observed from the paper that GA optimization algorithm gives a SLL of -34.5dB with excitation amplitude optimization. Applying same constraints as mentioned in [23] with DE algorithm having parameters as mentioned in Table3.1, it is observed from fig. 3.4 that SLL reaches a value of -38.42dB for amplitude variation as indicated in Table 3.2.

Table 3.1: Parameters Used for DE Validation

S No.	Parameters	Value
1	Number of Elements	24
2	Inter-element Spacing	0.5λ
3	Population Size	50
4	Iterations	1000
5	θ_{MLL}	(76,104)
6	θ_{SLL}	[0,76]&[104,180]
7	F	0.8
	CR	0.3
	VTR	0

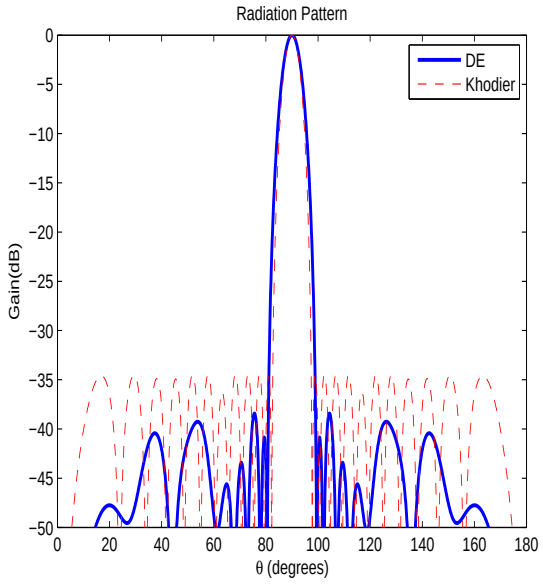

(a) Radiation Pattern Comparision

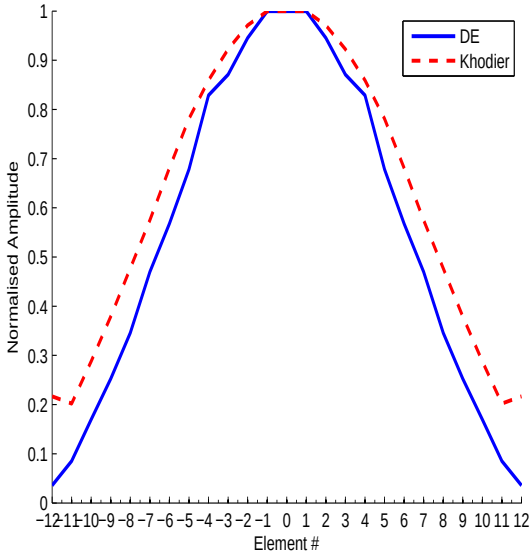

(b) Normalized amplitude distribution $|I_n|$ of array elements

Figure 3.4: DE and PSO(Khodier) for N=24 Symmetric Linear Array

Table 3.2: Performance Comparison between DE and PSO (Khodier)

Algorithms	Normalised Amplitude(I_n)	SLL(in dB)
PSO(Khodier)	1.0000,0.9712,0.9226,0.8591,0.7812,0.6807 0.5751,0.4768,0.3793,0.2878,0.2020,2167	-34.5
DE	1.0000,0.9454,0.8709,0.8288,0.6783,0.5676 0.4699,0.3457,0.2525,0.1695,0.0852,0.0355	-38.42

3.2.2 Simplified Swarm Optimization Algorithm

Simplified Swarm optimization(SSO) is an emerging met-heuristic algorithm which searches for best values with the help of population (swarm) of individuals (particles) which gets updated to better values with each iterations. It is derived from Particle Swarm optimization(PSO), as a simplified version of PSO technique It is designed to remove the premature convergence of PSO in high-dimensional multi-modal problems [8, 9]. Thus, SSO is able to improve the convergence speed with increase in number of iterations. SSO starts with some size of swarm population having random position of particles, maximum number of generations and three controlling parameters C_w, C_p & C_g depending on the application. In every generation, the particle's position value in each dimension keeps on updating to some new pbest value or gbest value or some random value according to following criteria as under [8]:

$$x_{id}^{t} = \begin{cases} x_i^{t-1}, & \text{if rand}() \in [0, C_w) \\ p_i^{t-1}, & \text{if rand}() \in [C_w, C_p) \\ g_i^{t-1}, & \text{if rand}() \in [C_p, C_g) \\ x, & \text{if rand}() \in [C_g, 1) \end{cases}$$

here, i=1,2,.....m; where m is size of swarm

$$X_i = (x_{i1}, x_{i1}, \ ..... \ x_{iD})$$

where, x_{iD} is the position value of the i_{th} particle for D_{th} space dimension. C_w, C_p & C_g are three constant positive parameters such that

$$C_w \ < \ C_p \ < \ C_g$$

$P_i = (p_{i1}, p_{i1}, \ ..... \ p_{iD})$ denotes the best solution achieved by each individuals (pbest),
$G_i = (g_{i1}, g_{i1}, \ ..... \ g_{iD})$ denotes the best solution achieved so far by the whole swarms (gbest),
x represents the new value for the particle in every dimension which are randomly generated from random function 'rand()'; where, the random number can be taken between 0 and 1.
The SSO algorithm is explained in detail by the flowchart fig. 3.5 shown below:

Validation of SSO

Referred to AF of circular array [14] of 30 isotropic elements with inter-element spacing of 0.5λ, optimization based on SSO algorithm has been applied under mentioned constraints and compared with GA results to show the superiority of SSO over GA. The various parameters considered for this comparison [14] are shown in Table 3.3. It is observed from the simulated result fig. 3.6 & Table 3.4 that there is a drastic reduction in side lobe level which reduces from -10.88dB with Genetic algorithm used in [14] to a value of -13.11dB with the proposed SSO algorithm. Moreover, no ripples are observed with proposed scheme showing an upper hand of the proposed scheme.

Table 3.3: Parameters Used for SSO Validation

S No.	Parameters	Value
1	Number of Elements	30
2	Inter-element Spacing	0.5λ
3	Population Size	50
4	Iterations	500
5	θ_{CSC}	(0,30)
6	θ_{SLL}	(-90,0)&(30,90)
7	C_g C_p C_w	[0.45,0.65] (0.65,0.85] (0.85,0.95]

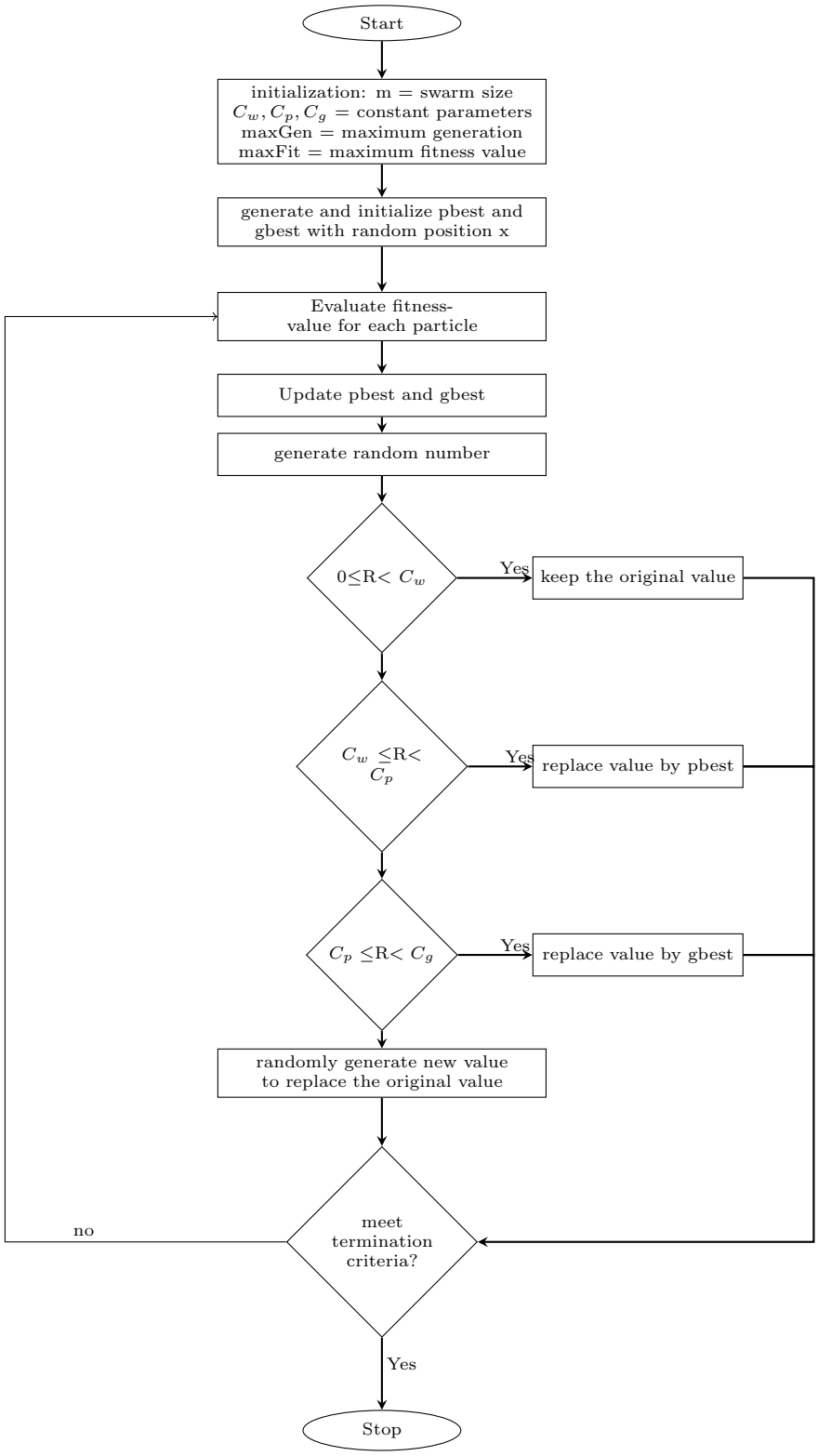

Figure 3.5: Flowchart of SSO Algorithm

Table 3.4: Desired & Obtained Results

Parameter	Desired	GA	SSO
SLL(in dB)	-15	-10.88	-13.11

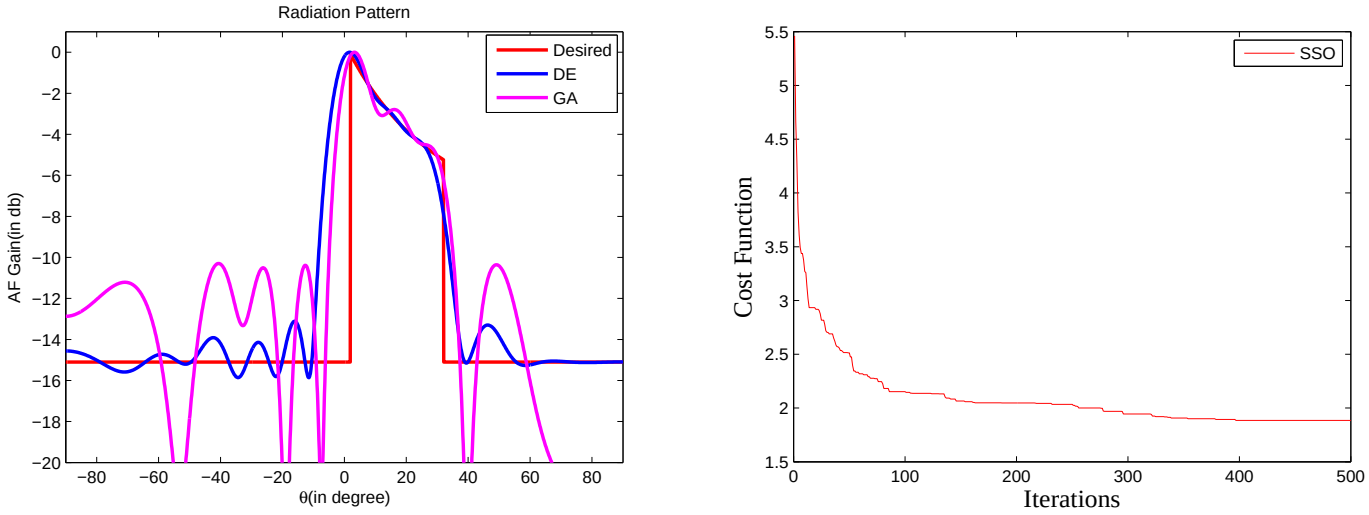

(a) Radiation Pattern

(b) SSO Cost Function

Figure 3.6: Comparison Result between SSO & GA for N=30 Circular Array

3.3 Simulation Results for Cosecant Square Pattern

Applying basic Differential evolution(DE) and Simple Swarm optimization(SSO) algorithms on linear, circular and spherical array, cosecant-squared pattern is generated. The desired pattern used for all three conformal arrays is as shown in fig.3.7 is plotted against azimuthal angle ϕ with a cosecant-squared curve of 45°.

The calculation of ripple component in the obtained $cosec^2$ pattern is given by cumulative summation of the deviation Δ_{ripple} in cosecant curve from desired curve as :

$$\Delta_{ripple} = \Delta_{CSC} = \sum_{\theta \in [cscrange]} |AF(\theta, 90) - Desired(\theta, 90)| \qquad (3.6)$$

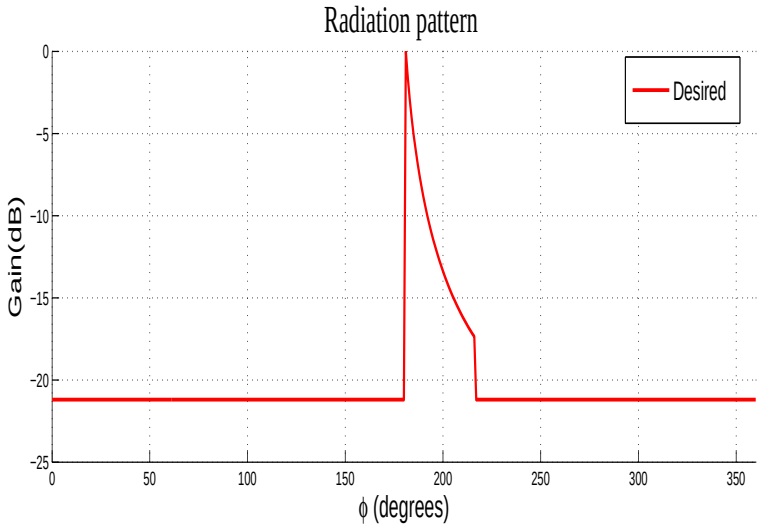

Figure 3.7: Desired CSP for all three Conformal Antenna Array

3.3.1 Case Study 1: Spherical Array

An array factor of spherical array with 184,260 & 376 isotropic elements placed such that 26,34 & 50 elements are in main circular array, 156, 224 &324 elements are arranged in twelve sub-circular arrays and single element is at the top and the bottom as in equation (4.1) with I_{nm} optimization is considered:

$$AF_{sph}(\theta,\phi) = \sum_{m=-M}^{M}\sum_{n=1}^{N_m} I_{nm} exp^{(jka_m sin(\theta)cos(\phi-\phi_{nm})+j\psi_n)+(jkd_m cos(\theta)+\beta_m)} + exp^{(jka_0\cos\theta)} + exp^{(-jka_0\cos\theta)} \quad (3.7)$$

where,

$I_{nm} = |Inm|e^{j\psi_n}$ is the current excitation for n^{th} antenna element of m^{th} circular array,

$|I_{nm}|$ is the normalised amplitude and ψ_n is the phase of excitation,

ϕ_{nm} is the azimuth position of n^{th} antenna element on m^{th} circular array,

a_m is the radius for m^{th} circle of spherical array,

a_0 is the radius of spherical array,

d_m is the distance of m^{th} circular array from reference circular array at the origin,

The fitness function used for spherical array is given by equation as:

$$f_{cost} = \alpha * \Delta_{CSC} + \beta * \Delta_{SLL} + \gamma * \Delta \tag{3.8}$$

where, $\Delta = \sum_{\phi\in[0,360]} |AF(90,\phi) - Desired(90,\phi)|$
$\Delta_{CSC} = \sum_{\phi\in[181,225]} |AF(90,\phi) - Desired(90,\phi)|$
$\Delta_{SLL} = \sum_{\phi\in[0,180]\&[226,360]} |AF(90,\phi) - Desired(90,\phi)|$
To reduce the ripple in main lobe level the values of $\alpha, \beta and \gamma$ values are taken as 0.875,0.125 and 0.00 respectively.

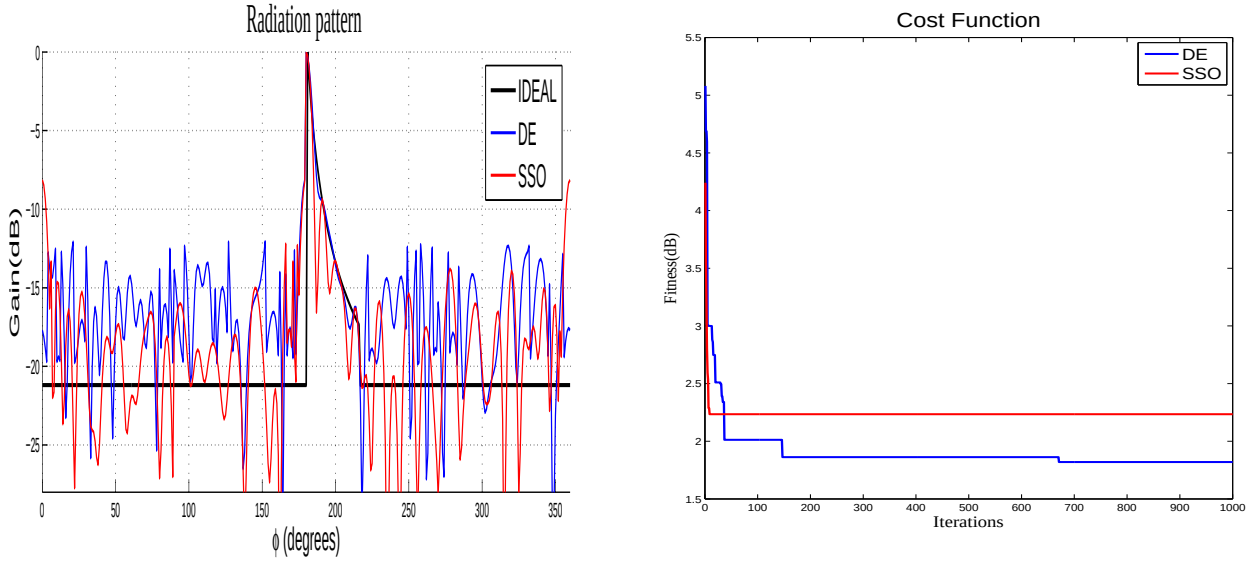

(a) Radiation Pattern for N=376 Elements

(b) Cost Function for N=376 Elements

Figure 3.8: Results of Spherical Array with 376 elements

From the simulation results fig 3.8, fig.3.9 & fig.3.10 it can be understand that cosecant squared pattern is synthesised well in main lobe by using spherical antenna array with different number of elements.
From the cost function figures shows that the amount of convergence is not following particular relation with the number of elements. From all the three figures it is clear that the rate of convergence for sso algorithm is better than the de algorithm.
The amount of convergence between DE and SSO is incomparable as it is different for different set of elements.

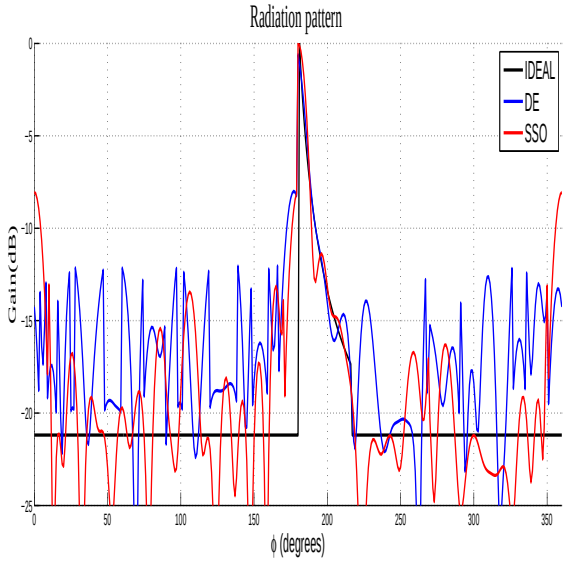

(a) Radiation Pattern for N=260 Elements

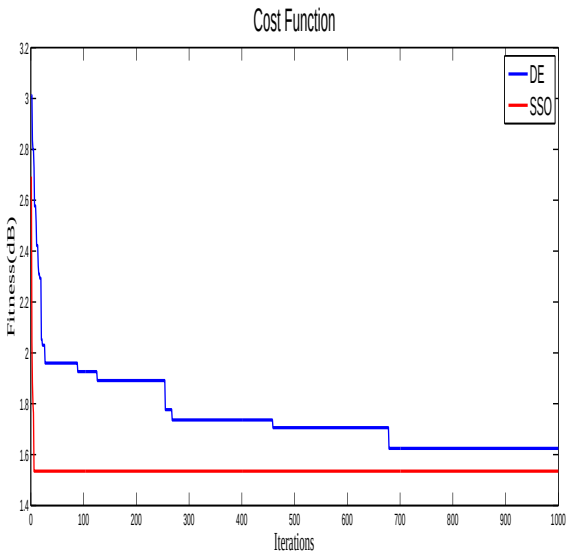

(b) Cost Function for N=260 Elements

Figure 3.9: Results of Spherical Array with 260 elements

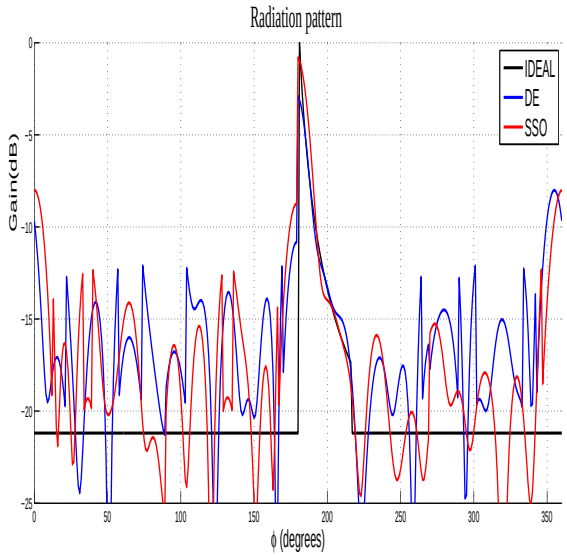

(a) Radiation Pattern for N=184 Elements

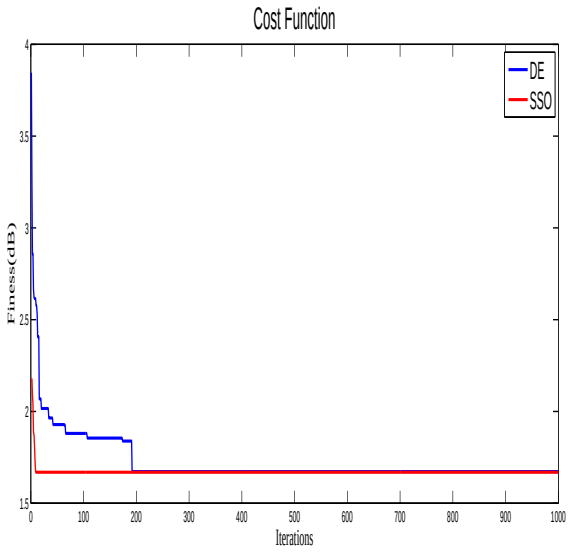

(b) Cost Function for N=184 Elements

Figure 3.10: Results of Spherical Array with 184 elements

3.3.2 Case Study 2: Cylindrical Array

An array factor of cylindrical array with 182,286 & 390 isotropic elements placed such that 14,22 & 30 elements are in each circular array. A linear arrangement of 13 such circular arrays is as in equation (3.9) with I_{nm} opti-

mization is considered:

$$AF_{cyl}(\theta,\phi) = \sum_{m=-M}^{M}\sum_{n=1}^{N} I_{nm} exp^{(jkrsin(\theta)cos(\phi-\phi_{nm})+j\psi_m)+(jkd_m cos(\theta)+\beta_m)} \quad (3.9)$$

where,
$I_{nm} = |Inm|e^{j\psi_n}$ is the current excitation for n^{th} antenna element of m^{th} circular array,
$|I_{nm}|$ is the normalised amplitude and ψ_n is the phase of excitation,
ϕ_{nm} is the azimuth position of n^{th} antenna element on m^{th} circular array,
r is the radius of cylindrical array,
d_m is the distance of m^{th} circular array from reference circular array at the origin,
The fitness function used for spherical array is given by equation as:

$$f_{cost} = \alpha * \Delta_{CSC} + \beta * \Delta_{SLL} + \gamma * \Delta \quad (3.10)$$

where, $\Delta = \sum_{\phi\in[0,360]} |AF(90,\phi) - Desired(90,\phi)|$
$\Delta_{CSC} = \sum_{\phi\in[181,225]} |AF(90,\phi) - Desired(90,\phi)|$
$\Delta_{SLL} = \sum_{\phi\in[0,180]\&[226,360]} |AF(90,\phi) - Desired(90,\phi)|$
To reduce the ripple in main lobe level the values of $\alpha, \beta and \gamma$ values are taken as 0.875,0.125 and 0.00 respectively.

It is observed from the simulation results fig 3.11, fig3.12 & fig 3.13 that it can be understand that cosecant squared pattern is synthesised well in main lobe by using cylindrical antenna array with different number of elements. From the cost function figures it is clear that as the number of elements decreases, the better cosecant square radiation pattern is achieved.
From all the three figures it is clear that the rate of convergence is better for sso algorithm and amount of convergence is better for DE.

3.3.3 Case Study 3: Conical Array

An array factor of conical array with 195,291 & 381 isotropic elements placed such that 32,44 & 56 elements are in main circular array and 162, 246 & 324

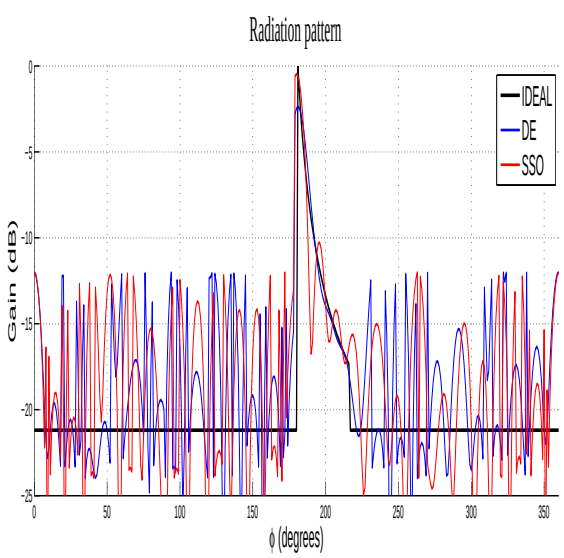

(a) Radiation Pattern for N=390 Elements

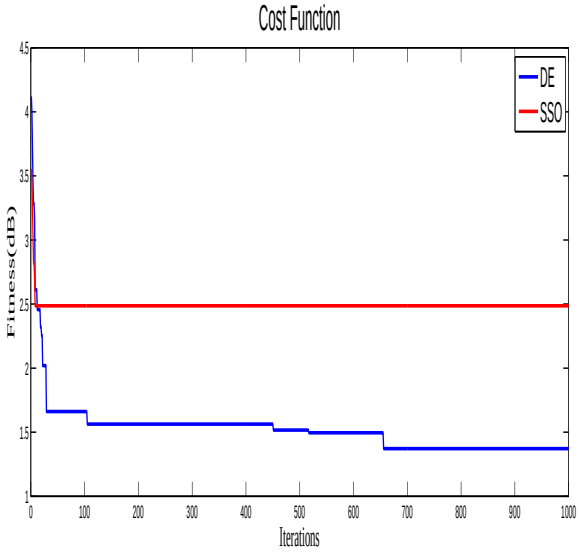

(b) Cost Function for N=390 Elements

Figure 3.11: Results of Cylindrical Array with 390 elements

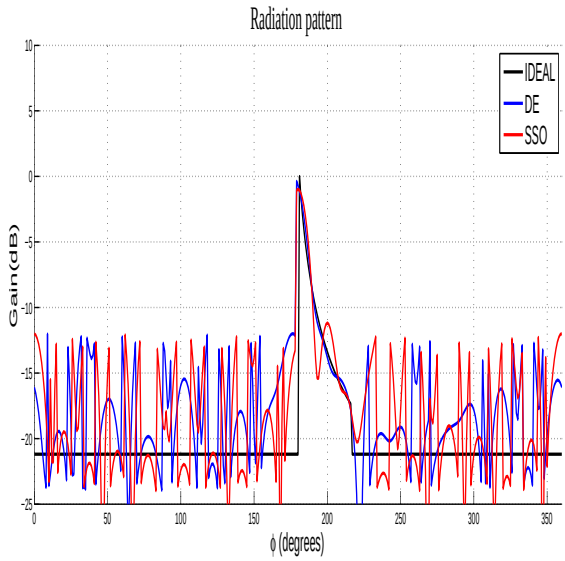

(a) Radiation Pattern for N=286 Elements

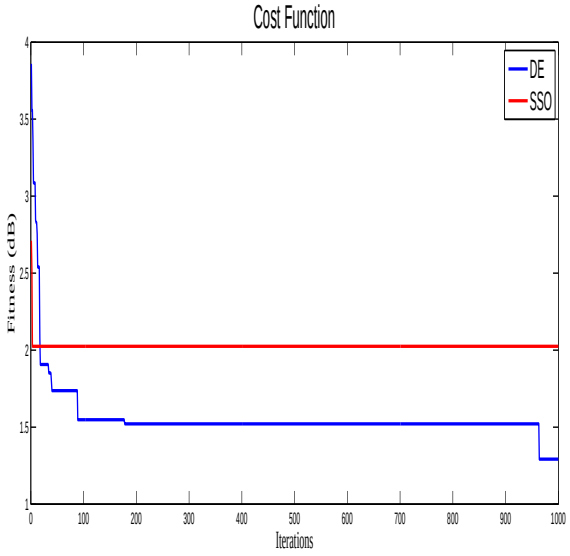

(b) Cost Function for N=286 Elements

Figure 3.12: Results of Cylindrical Array with 286 elements

elements are arranged in twelve sub-circular arrays and single element is at the vertex as in equation (4.3) with I_{nm} optimization is considered:

$$AF_{con}(\theta,\phi) = \sum_{m=1}^{M}\sum_{n=1}^{N_m} I_{nm} exp^{(jkr_m sin(\theta)cos(\phi-\phi_{nm})+j\psi_n)+(jkd_m cos(\theta)+\beta_m)} + exp^{(-jkh\cos\theta)} \tag{3.11}$$

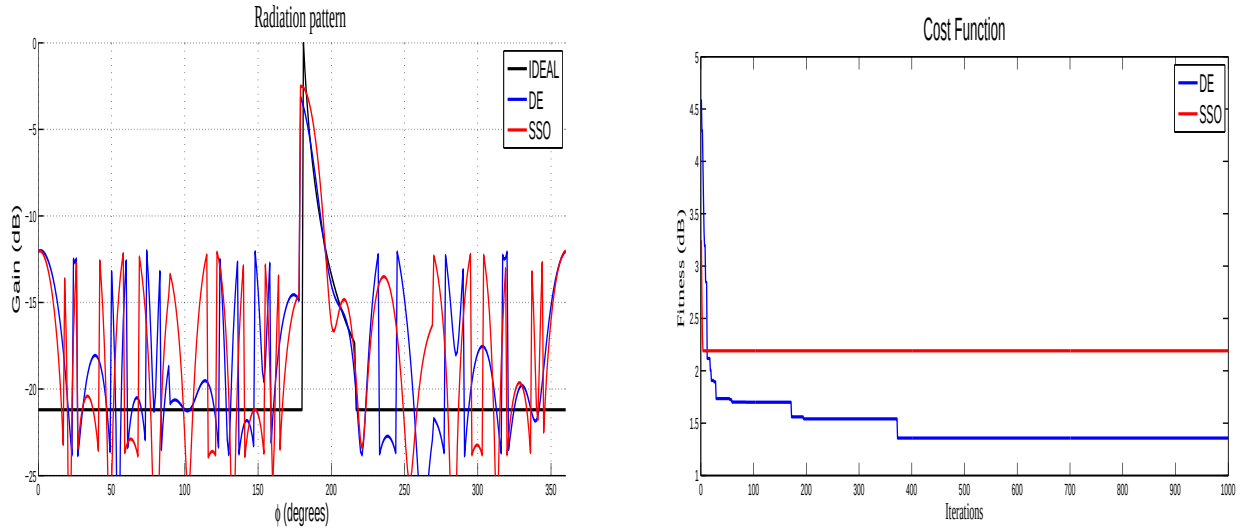

(a) Radiation Pattern for N=182 Elements

(b) Cost Function for N=182 Elements

Figure 3.13: Results of Cylindrical Array with 182 elements

where,

$I_{nm} = |Inm|e^{j\psi_n}$ is the current excitation for n_{th} antenna element of m_{th} circular array,

$|I_{nm}|$ is the normalised amplitude and ψ_n is the phase of excitation,

ϕ_{nm} is the azimuth position of n_{th} antenna element on m_{th} circular array,

r_m is the radius for m_{th} circle of conical array,

h is the height of conical array,

d_m is the distance of m_{th} circular array from reference circular array at the origin,

The fitness function used for conical array is given by equation as:

$$f_{cost} = \alpha * \Delta_{CSC} + \beta * \Delta_{SLL} + \gamma * \Delta \tag{3.12}$$

where, $\Delta = \sum_{\phi\in[0,360]} |AF(90,\phi) - Desired(90,\phi)|$

$\Delta_{CSC} = \sum_{\phi\in[181,225]} |AF(90,\phi) - Desired(90,\phi)|$

$\Delta_{SLL} = \sum_{\phi\in[0,180]\&[226,360]} |AF(90,\phi) - Desired(90,\phi)|$

To reduce the ripple in main lobe level the values of $\alpha, \beta and \gamma$ values are taken as 0.875,0.125 and 0.00 respectively.

The simulation results in fig 3.14, fig3.15 & fig3.16 shows that the squared

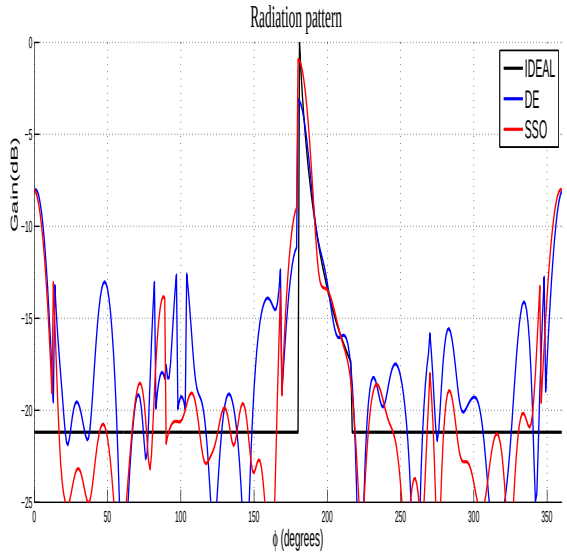

(a) Radiation Pattern for N=381 Elements

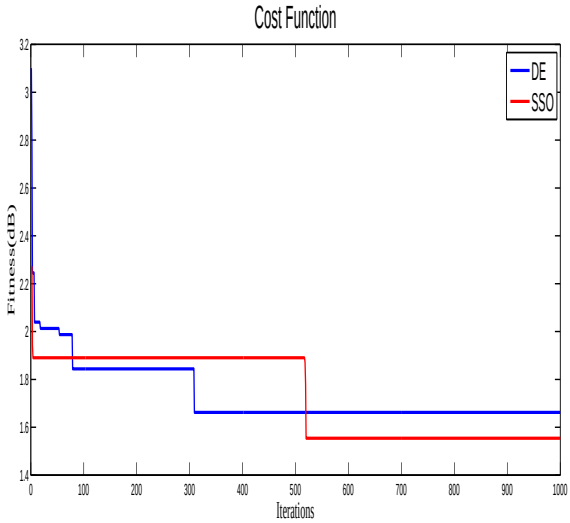

(b) Cost Function for N=381 Elements

Figure 3.14: Results of Conical Array with 381 elements

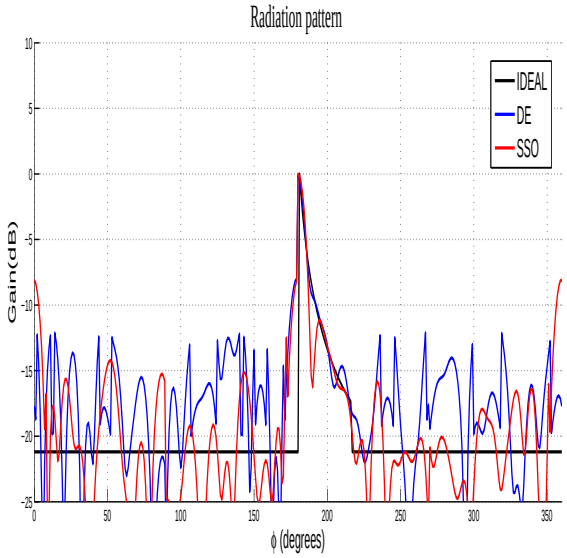

(a) Radiation Pattern for N=291 Elements

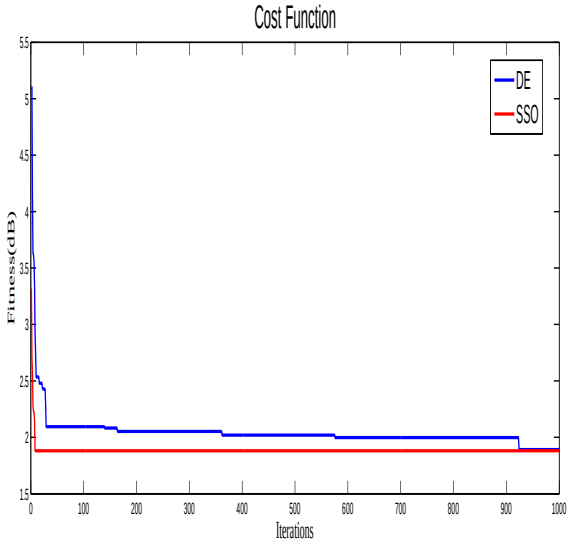

(b) Cost Function for N=291 Elements

Figure 3.15: Results of Conical Array with 291 elements

pattern is synthesised better in main lobe by using conical antenna array with different number of elements.

From the cost function figures it is clear that as the number of elements increases the better cosecant square radiation pattern is achieved.

But the amount of convergence and rate of convergence doesnt follow any relation between DE and SSO.

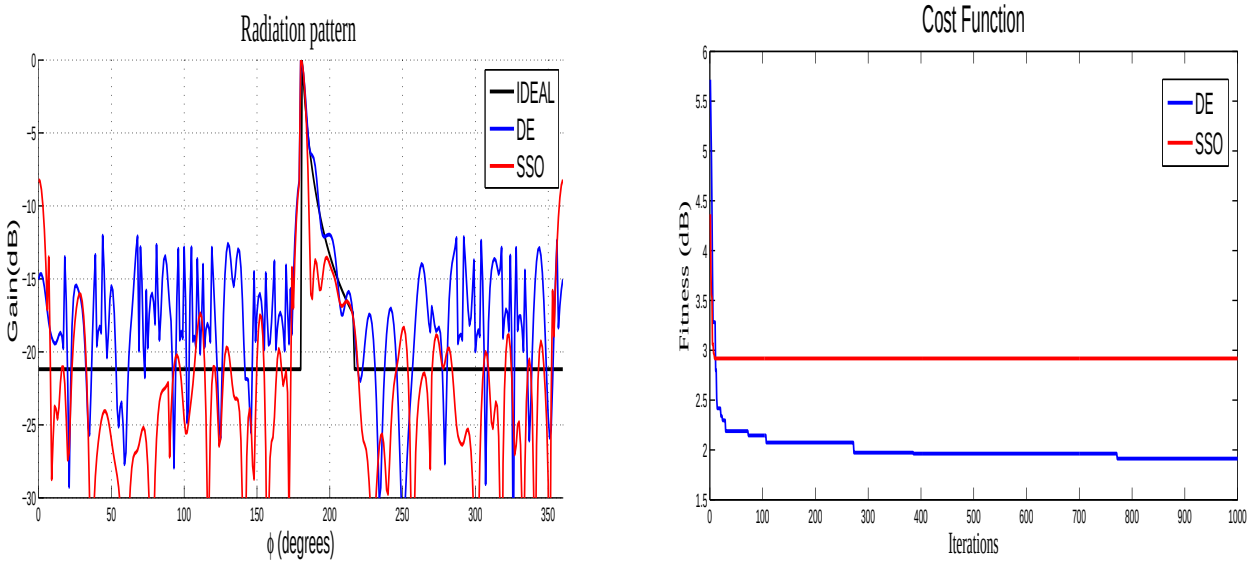

(a) Radiation Pattern for N=195 Elements

(b) Cost Function for N=195 Elements

Figure 3.16: Results of Conical Array with 195 elements

Table 3.5: Performance Comparison of Conformal arrays

comparison Parameter	Spherical Array as No. of Elements increases	Cylindrical Array as No. of Elements increases	Conoical Array as No. of Elements increases
Rate of convergence w.r.t No. of elements	SSO > DE	SSO > DE	– – –
Amount of convergence w.r.t No. of elements	– – –	Decreases	Increases
Amount of convergence w.r.t algorithms	– – –	DE > SSO	– – –

where – – – indicates there is no particular trend.

Chapter 4

Impact of Azimuthal Plane Elements

4.1 Problem Formulation

The cosecant squared pattern is synthesized by linear antenna array [13] and also by conformal antenna arrays.There is a significant difference in number of elements in linear and conformal array for the generation of cosecant squared radiation pattern. To bridge this gap, only elements in an azimuthal plane of conformal antenna array are excited based on the mask generated for that azimuthal plane constraint, and the cosecant squared radiation pattern is synthesized. The excitation parameters of the conformal array elements are optimized using DE & SSO optimization techniques.

4.2 Selection of Azimuthal Plane

For selecting the elements in azimuthal plane,the position coordinates of the existing elements are used to generate the mask and masking is done for the elements. The procedure for selecting the azimuthal plane for best radiation pattern is as shown in flowchart.

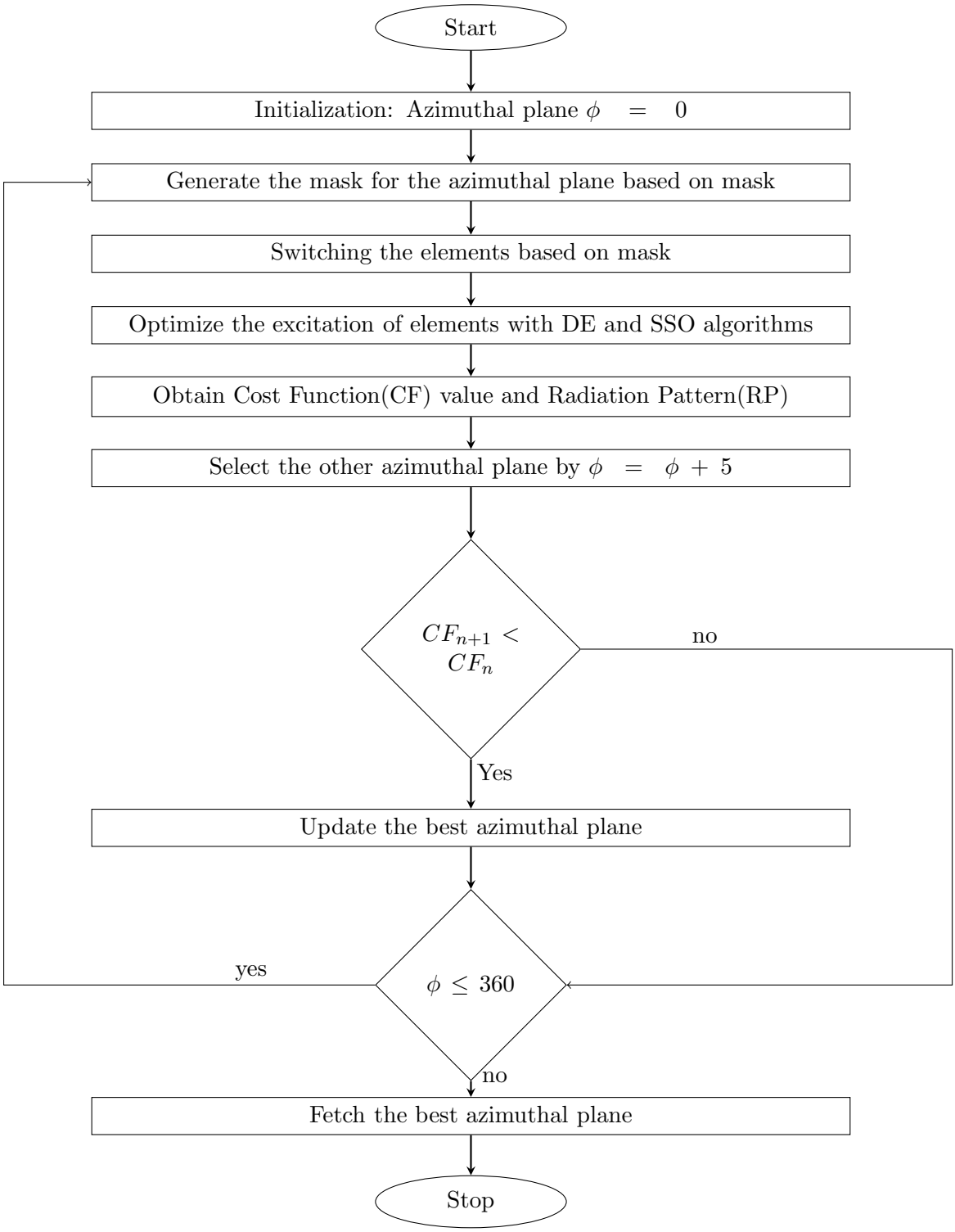

Figure 4.1: Procedure for Selection of Best Azimuthal Plane

4.3 Pattern Synthesis with Different Azimuthal Plane Elements

4.3.1 Case1: Spherical Array

For selecting the elements in azimuthal plane,the position coordinates of the existing elements are used to generate the mask and masking is done for the elements. The procedure for selecting the azimuthal plane for best radiation pattern is as shown in fig.4.1.E is the mask generated for the ϕ plane which generates the radiation pattern closer to the desired pattern.The array factor of the spherical array with the selected elements is the product of masking coefficient and the spherical array factor as in equation 4.1 and final equation is given as

$$AF_{sph}(\theta,\phi) = \sum_{m=-M}^{M}\sum_{n=1}^{N_m} E_{nm} * I_{nm} exp^{(jka_m sin(\theta)cos(\phi-\phi_{nm})+j\psi_n)+(jkd_m cos(\theta)+\beta_m)} + exp^{(jka_0\cos\theta)} + exp^{(-jka_0\cos\theta)} \quad (4.1)$$

where E_{nm} is the masking coefficient for n^{th} antenna element of m^{th} circular array,

After masking, the selected elements of a particular azimuthal plane of the

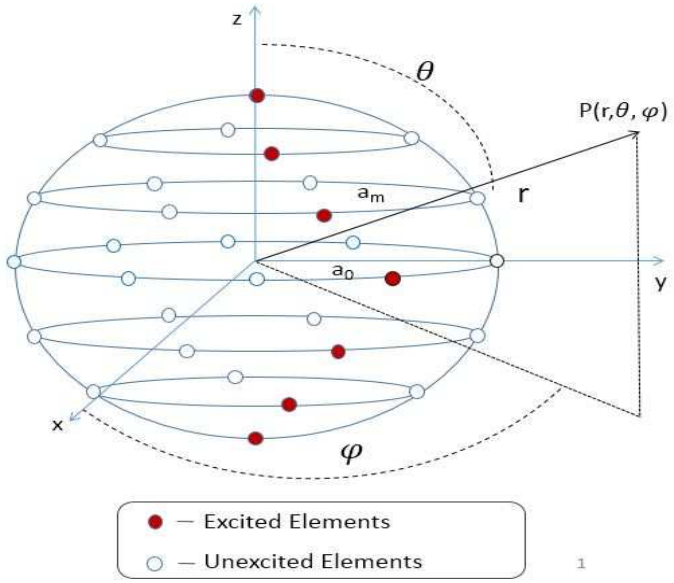

Figure 4.2: Spherical Antenna Array with Selection

spherical array can be viewed as shown in fig.4.2. The excitation parame-

ters of the selected elements are optimised using the DE and SSO algorithms.

Fig.4.3 and fig.4.4 are the simulation results when $\phi = 180°$ plane elements, $\phi = 355°$ plane elements got selected over the spherical array respectively. From the Fig.4.3 & FIg,4.4 it can easily noted that every ϕ plane selection will not be able to radiate the cosecant square pattern.

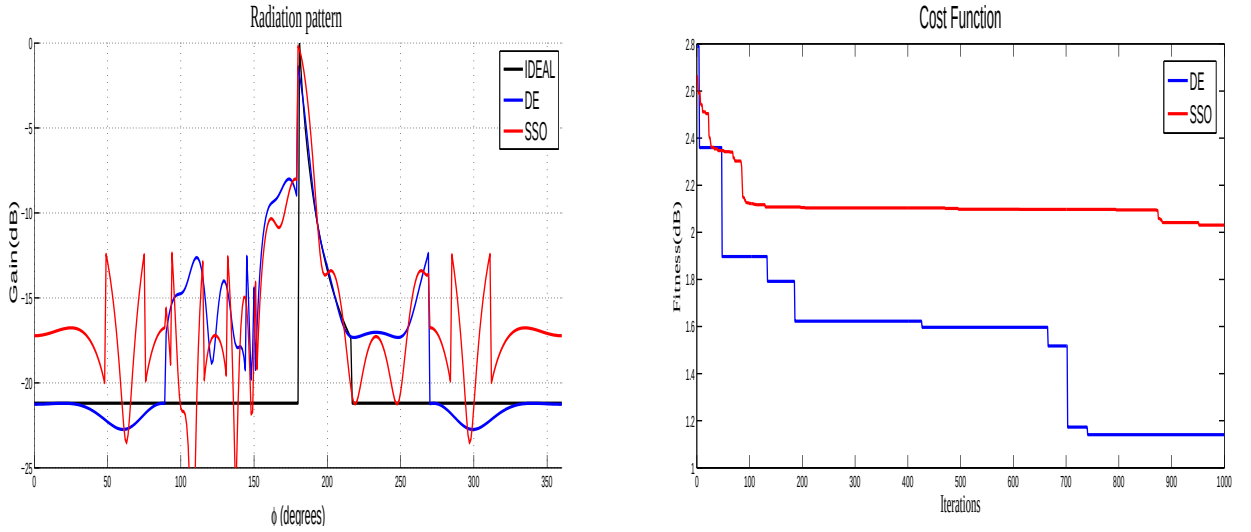

(a) Radiation Pattern for best ($phi = 180°$) Plane Elements (b) Cost Function for best ($phi = 180°$) Plane Elements

Figure 4.3: Results of Spherical Array for Best ($phi = 180°$) Plane Elements

From the Fig.4.3, clearly shows that the cosecant square pattern synthesis is done with the elments got selected over the $phi = 180°$ plane of the spherical array.

From the Fig.4.4,shows that the radiation pattern of the elments got selected over the $phi = 355°$ plane of the spherical array have more sidelobe levels and the main beam of CSP is also not synthesised.

4.3.2 Case2: Cylindrical Array

A mask is generated for the selection of elements of the cylindrical array in a particular ϕ plane with the procedure shown in flow chart4.1.E is the mask

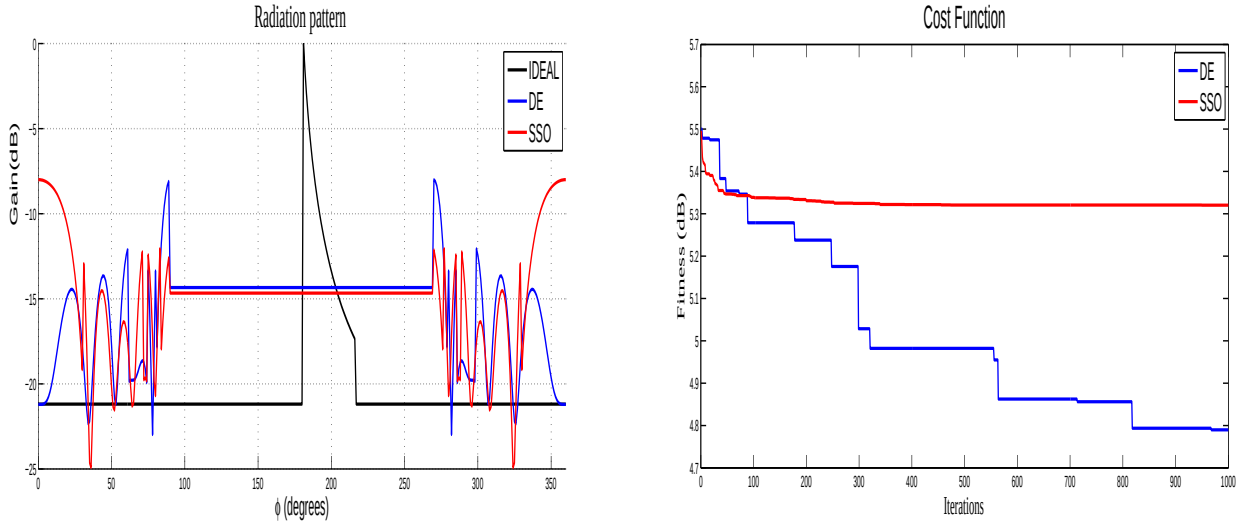

(a) Radiation Pattern for worst ($phi = 355°$) Plane Elements (b) Cost Function for worst ($phi = 355°$) Plane Elements

Figure 4.4: Results of Spherical Array for Worst ($phi = 355°$) Plane Elements

generated for the ϕ plane which generates the radiation pattern closer to the desired pattern.The array factor of the cylindrical array with the selected elements, is the product of masking coefficient and the cylindrical array factor as in equation 3.9 and final equation is given as

$$AF_{cyl}(\theta,\phi) = \sum_{m=-M}^{M}\sum_{n=1}^{N} E_{nm} * I_{nm} exp^{(jkrsin(\theta)cos(\phi-\phi_{nm})+j\psi_m)+(jkd_m cos(\theta)+\beta_m)} \tag{4.2}$$

where E_{nm} is the masking coefficient for n^{th} antenna element of m^{th} circular array,

The finally selected elements are of desired azimuthal plane as shown in Fig. 4.5 for cylindrical array.The excitation parameters of the selected elements are optimised using the DE and SSO algorithms.

Fig.4.6 and fig.4.7 are the simulation results when $\phi = 255°$ plane elements, $\phi = 0°$ plane elements got selected over the spherical array respectively. From the Fig.4.6 & FIg,4.7 it can easily noted that every ϕ plane selection will not be able to radiate the cosecant square pattern.

From the Fig.4.6, clearly shows that the cosecant square pattern synthesis

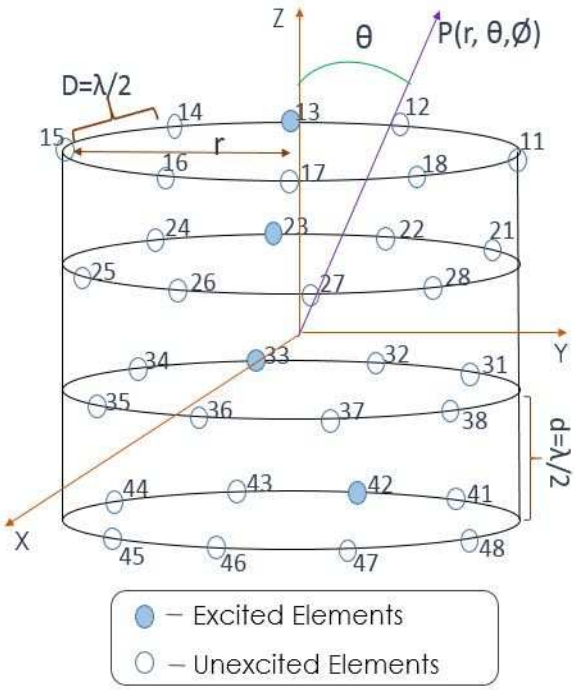

Figure 4.5: Cylindrical Antenna Array with Selection

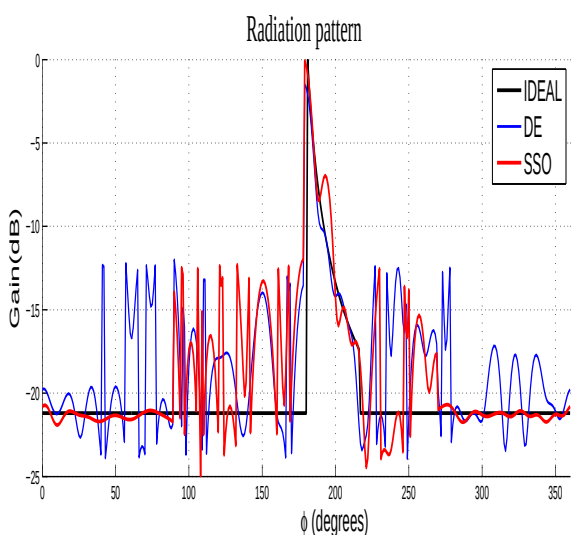

(a) Radiation Pattern for best ($phi = 255°$) Plane Elements

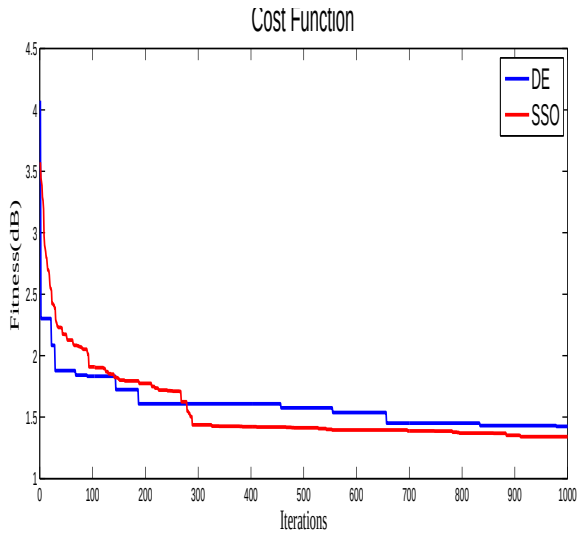

(b) Cost Function for best ($phi = 255°$) Plane Elements

Figure 4.6: Results of Cylindrical Array for Best ($phi = 255°$) Plane Elements

is done with the elements got selected over the $phi = 255°$ plane of the cylindrical array.

From the Fig.4.7,shows that the radiation pattern of the elements got

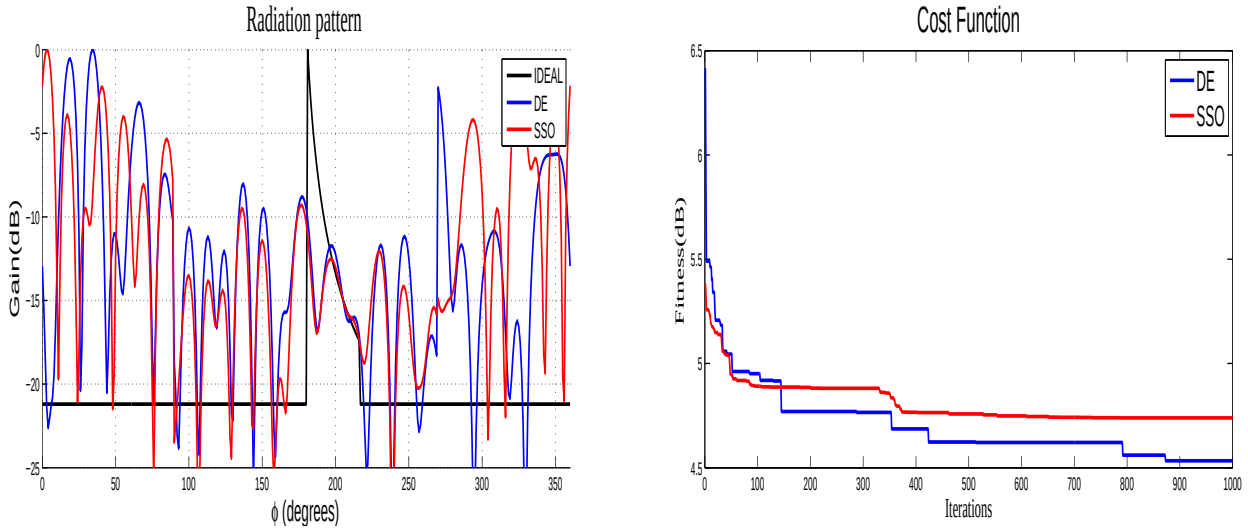

(a) Radiation Pattern for worst ($phi = 0°$) Plane Elements (b) Cost Function for worst ($phi = 0°$) Plane Elements

Figure 4.7: Results of Cylindrical Array for Worst ($phi = 0°$) Plane Elements

selected over the $phi = 0°$ plane of the cylindrical array have more side lobe levels and the main beam of CSP is also not synthesised.

4.3.3 Case3: Conical Array

For selecting the elements in azimuthal plane,the position coordinates of the existing elements are used to generate the mask and masking is done for the elements. The procedure for selecting the azimuthal plane for best radiation pattern is as shown in fig.4.1.E is the mask generated for the ϕ plane which generates the radiation pattern closer to the desired pattern.The array factor of the conical array with the selected elements is the product of masking coefficient and the conical array factor as in equation 4.3 and final equation is given as

$$AF_{con}(\theta,\phi) = \sum_{m=1}^{M}\sum_{n=1}^{N_m} E_{nm} I_{nm} exp^{(jkr_m sin(\theta) cos(\phi-\phi_{nm})+j\psi_n)+(jkd_m cos(\theta)+\beta_m)} + exp^{(-jkh\cos\theta)} \tag{4.3}$$

where E_{nm} is the masking coefficient for n^{th} antenna element of m^{th} circular array,

The finally selected elements are of desired azimuthal plane as shown in Fig. 4.8 for conical array.The excitation parameters of the selected elements are

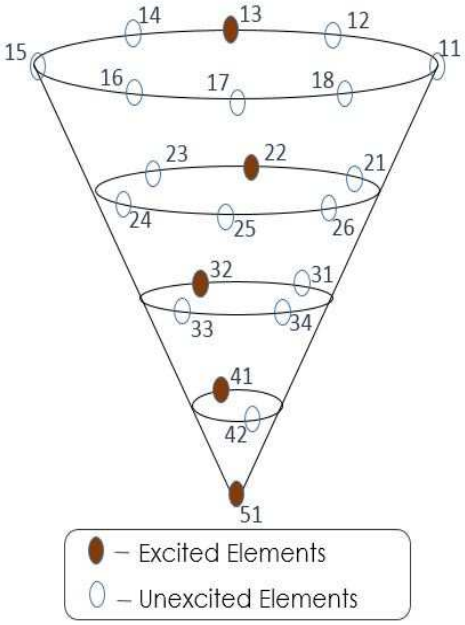

Figure 4.8: Conical Antenna Array with Selection

optimised using the DE and SSO algorithms.

Fig.4.9 and fig.4.10 are the simulation results when $\phi = 175^\circ$ plane elements, $\phi = 60^\circ$ plane elements got selected over the spherical array respectively. From the Fig.4.9 & Fig,4.10 it can easily noted that every azimuthal plane selection will not be able to radiate the cosecant square pattern.

From the Fig.4.9, clearly shows that the cosecant square pattern synthesis is done with the elements got selected over the $phi = 175^\circ$ plane of the cylindrical array.

From the Fig.4.10,shows that the radiation pattern of the elements got selected over the $phi = 60^\circ$ plane of the cylindrical array have more side lobe levels and the main beam of CSP is also not synthesised.

4.4 Pattern Synthesis with Best Azimuthal Plane Elements

4.4.1 Case4: Spherical Array with different set of elements

The procedure for selecting the azimuthal plane for best radiation pattern is as shown in fig.4.1, is done for the spherical antenna array with 260 and 184

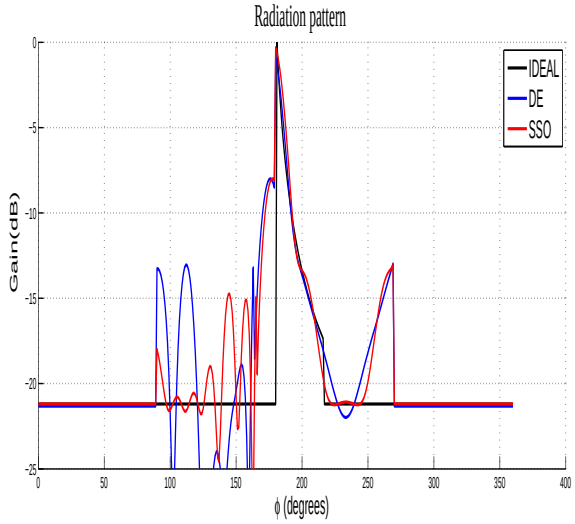

(a) Radiation Pattern for best ($phi = 175°$) Plane Elements

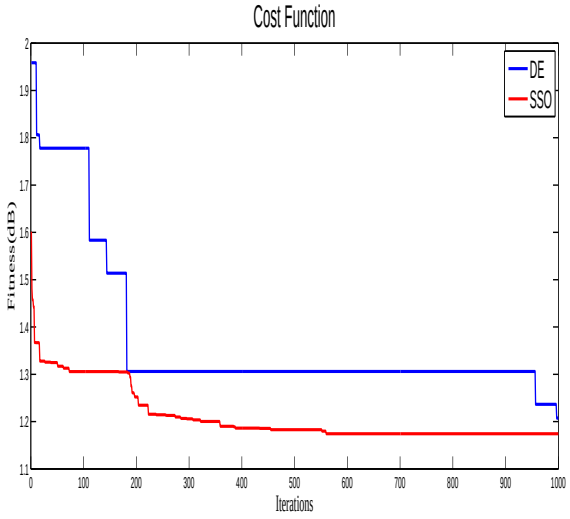

(b) Cost Function for best ($phi = 175°$) Plane Elements

Figure 4.9: Results of Conical Array for Best ($phi = 175°$) Plane Elements]

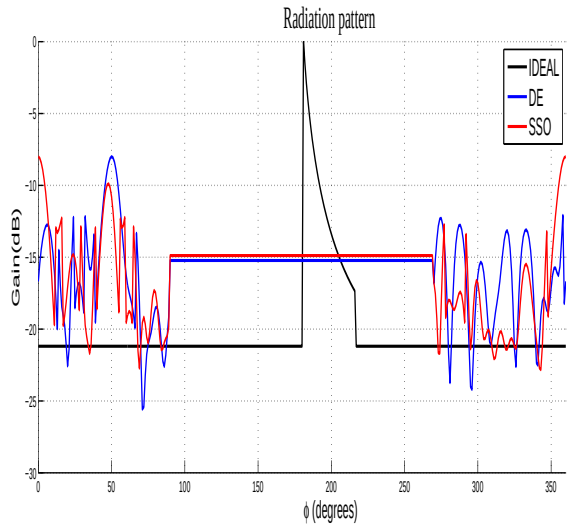

(a) Radiation Pattern for worst ($phi = 60°$) Plane Elements

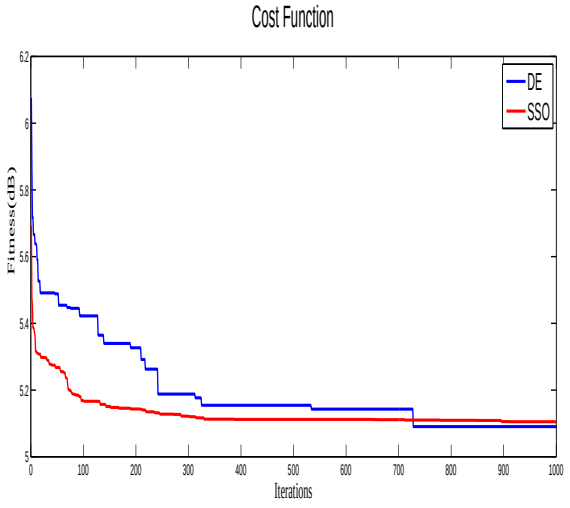

(b) Cost Function for worst ($phi = 175°$) Plane Elements

Figure 4.10: Results of Conical Array for Worst ($phi = 60°$) Plane Elements]

number of elements on it.

Fig.4.11 & Fig.4.12 shows the results for the best azimuthal plane ($phi = 180°$) selection of spherical antenna array with total number of elements as 260 & 184 respectively.

From the Fig.4.11 & Fig.4.12 it is clearly observed that DE optimization is better in amount of convergence and the SSO optimization is better in rate of convergence.

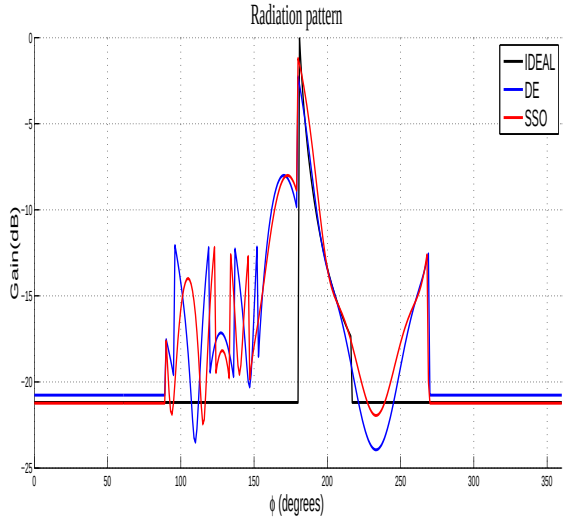

(a) Radiation Pattern for best ($phi = 180°$) Plane Elements

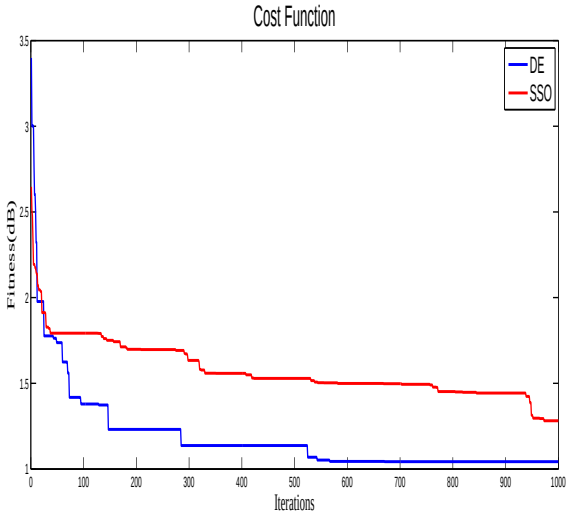

(b) Cost Function for best ($phi = 180°$) Plane Elements

Figure 4.11: Results of Spherical Array for Best ($phi = 180°$) Plane Elements

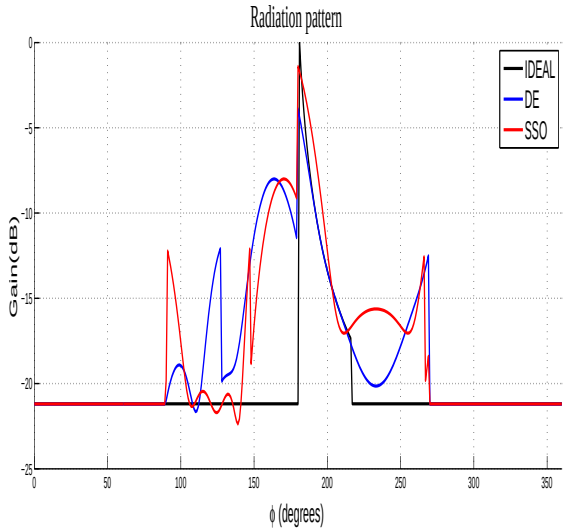

(a) Radiation Pattern for best ($phi = 180°$) Plane Elements

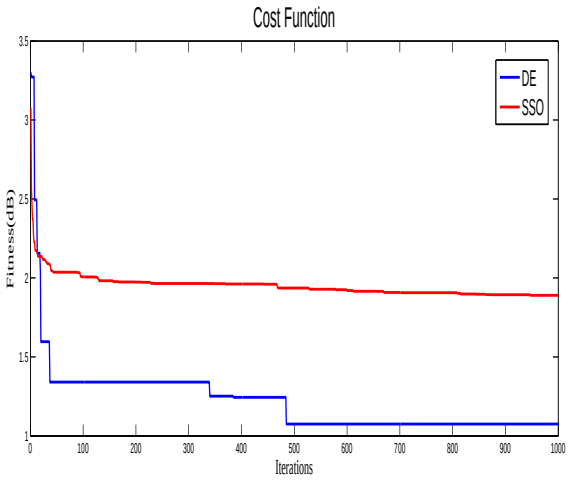

(b) Cost Function for best ($phi = 180°$) Plane Elements

Figure 4.12: Results of Spherical Array for Best ($phi = 180°$) Plane Elements

4.4.2 Case5: Cylindrical Array with different set of elements

The procedure for selecting the azimuthal plane for best radiation pattern is as shown in fig.4.1, is done for the cylindrical antenna array with 286 and 182 number of elements on it.

Fig.4.13 & Fig.4.14 shows the results for the best azimuthal plane ($phi = 255°$) selection of cylindrical antenna array with total number of elements as 286 & 182 respectively.

Table 4.1: Performance Comparison for Spherical Array

all elements seletion			$phi = 180°$ selected		
No. of ele.	DE ripple(dB)	SSO ripple(dB)	No. of ele.	DE ripple(dB)	SSO ripple(dB)
376	0.6411	0.9733	13	0.2387	0.7215
260	0.7524	0.9639	12	0.286	0.8218
184	0.9	1.02	12	0.2468	0.789

Fig.4.13 clearly shows that the amount of convergence for both DE and SSO

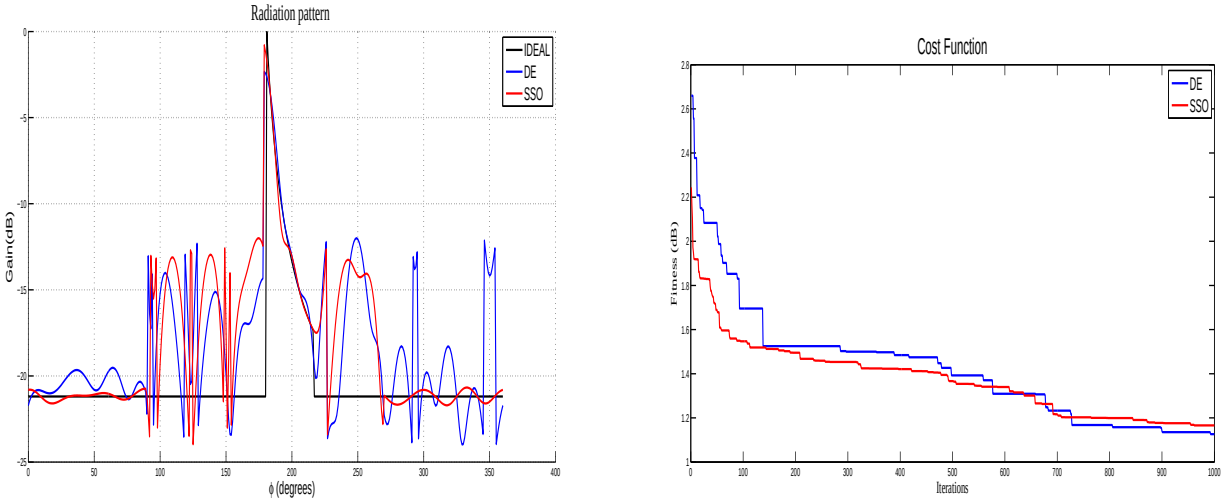

(a) Radiation Pattern for best ($phi = 255°$) Plane Elements (b) Cost Function for best ($phi = 255°$) Plane Elements

Figure 4.13: Results of Cylindrical Array for Best ($phi = 255°$) Plane Elements

optimizations is approximately same for $phi = 255°$ Plane on cylindrical array with 286 elements.

Fig.4.14 clearly shows that the rate of convergence is better for SSO optimization than DE optimization for $phi = 255°$ Plane on cylindrical array with 182 elements.

Table 4.2: Performance Comparison for Cylindrical Array

all elements seletion			$phi = 255°$ selected		
No. of ele.	DE ripple(dB)	SSO ripple(dB)	No. of ele.	DE ripple(dB)	SSO ripple(dB)
390	0.6865	0.9454	13	0.285	1.0232
286	0.5127	0.846	12	0.3229	0.994
182	0.4131	0.8307	13	0.2208	0.8375

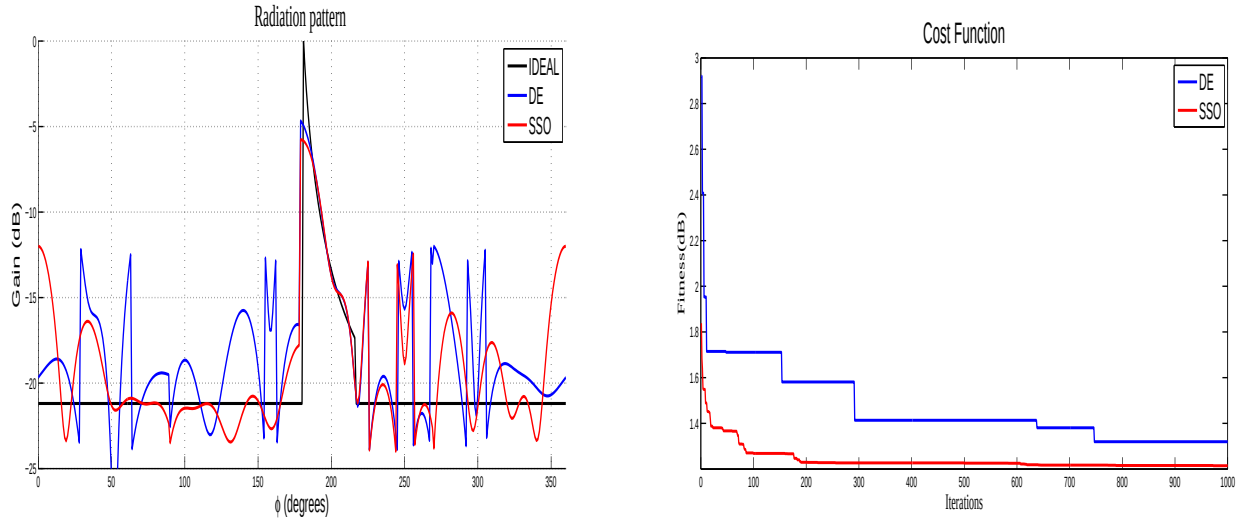

(a) Radiation Pattern for best ($phi = 255°$) Plane Elements (b) Cost Function for best ($phi = 255°$) Plane Elements

Figure 4.14: Results of Cylindrical Array for Best ($phi = 255°$) Plane Elements

4.4.3 Case6: Conical Array with different set of elements

The procedure for selecting the azimuthal plane for best radiation pattern is as shown in fig.4.1, is done for the conical antenna array with 291 and 195 number of elements on it.

Fig.4.15 & Fig.4.16 shows the results for the best azimuthal plane ($phi = 175°$) selection of cylindrical antenna array with total number of elements as 291 & 195 respectively.

Fig.4.15 clearly shows that the amount of convergence for both DE and SSO optimizations is approximately same for $phi = 175°$ Plane on conical array with 291 elements.

Fig.4.16 clearly shows that the rate of convergence is better for DE optimization than SSO optimization for $phi = 175°$ Plane on cylindrical array with 195 elements.

Table 4.3: Performance Comparison for Conical Array

all elements seletion			$phi = 175°$ selected		
No. of ele.	DE ripple(dB)	SSO ripple(dB)	No. of ele.	DE ripple(dB)	SSO ripple(dB)
381	0.9787	0.9899	13	0.3285	0.8706
291	0.9028	1.002	12	0.2347	0.8464
195	0.6409	0.9725	11	0.2639	0.7655

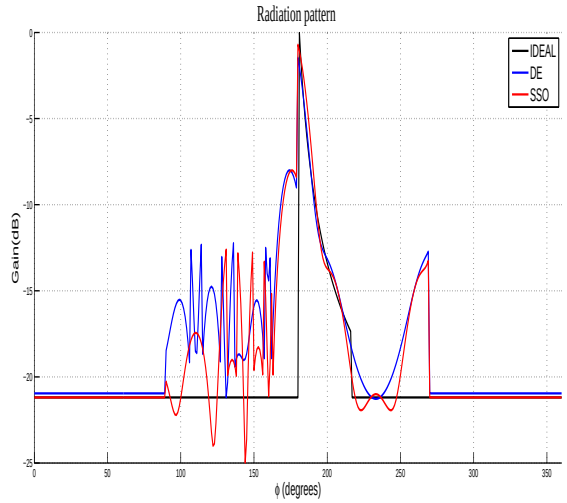

(a) Radiation Pattern for best ($phi = 175°$) Plane Elements

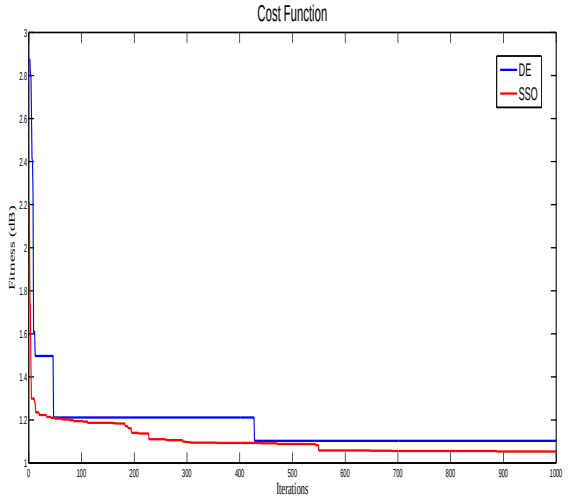

(b) Cost Function for best ($phi = 175°$) Plane Elements

Figure 4.15: Results of Conical Array for Best ($phi = 175°$) Plane Elements]

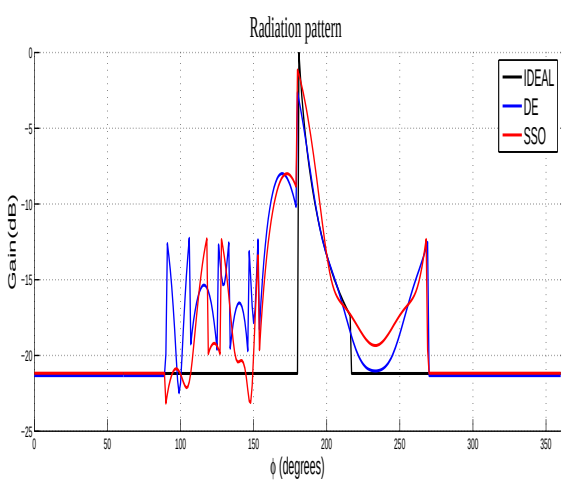

(a) Radiation Pattern for best ($phi = 175°$) Plane Elements

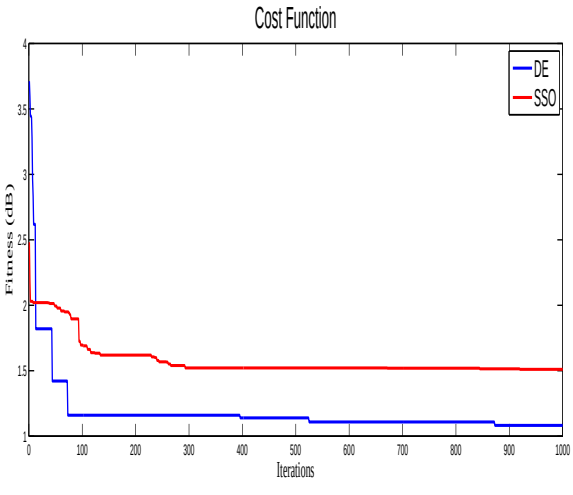

(b) Cost Function for best ($phi = 175°$) Plane Elements

Figure 4.16: Results of Conical Array for Best ($phi = 175°$) Plane Elements]

Chapter 5

Conclusion and Future Scope

5.1 Conclusions

- Formulation of conformal shapes like a spherical array, cylindrical array and the conical array with the concept of fundamental conventional arrays(Linear, Planar & Circular arrays).
- Synthesis of cosecant square pattern with a spherical array, cylindrical array and conical array by optimization of excitation parameters with DE ans SSO algorithms.
- Different azimuthal plane elements of spherical, cylindrical and conical antenna arrays are having different impact to get the desired radiation pattern.
- The best azimuthal plane for cosecant pattern synthesis is different for spherical, cylindrical and conical arrays.
- Simulation results concludes that reduction of ripple in the main lobe is achievable by less number of elements.

5.2 Limitations

- Isotropic Antenna elements which are theoretical are used in the generation of cosecant square pattern.
- Through out the work the mutual coupling between the antenna array elements is neglected.
- Mathematical simplification and formulation of array factor is valid only for the far field observations.
- Standard DE & SSO algorithms are applied for optimization to generate the desired patterns.

5.3 Future Scope

- Neuro fuzzy tools can be applied for the best possible weights of fitness function.
- Discussed cosecant square Shaped pattern can be generated using practical antenna as radiating element in the proposed conformal arrays.
- Further to achieve different radiation pattern, the constraints on the conformal arrays can be varied.
- Other algorithms nature and bio inspire can also be explored.

Bibliography

[1] Constantine A Balanis. *Antenna theory: analysis and design*. Wiley-Interscience, 2012.

[2] Robert S.Elliott. *ANTENNA THEORY AND DESIGN*. John Wiley and Sons, Ltd, 2005.

[3] Lars Josefsson and Patrik Persson. *Conformal array antenna theory and design*, volume 29. John wiley & sons, 2006.

[4] Jason Brownlee. *Clever Algorithms: Nature-Inspired Programming Recipes*. Jason Brownlee, 2011.

[5] Swagatam Das and Ponnuthurai Nagaratnam Suganthan. Differential evolution: A survey of the state-of-the-art. *Evolutionary Computation, IEEE Transactions on*, 15(1):4–31, 2011.

[6] Rainer Storn and Kenneth Price. Differential evolution a simple evolution strategy for fast optimization. *Dr. Dobb's*, (03):1824 and 78, April 1997.

[7] Rainer Storn and Kenneth Price. Differential evolution - a simple and efficient adaptive scheme for global optimization over continuous spaces. *Technical Report TR-95-012*, March 1995.

[8] Changseok Bae, Wei-Chang Yeh, Noorhaniza Wahid, Yuk Ying Chung, and Yao Liu. A new simplified swarm optimization (sso) using exchange local search scheme. *International Journal of Innovative Computing, Information and Control*, 8(6):4391–4406, 2012.

[9] S Revathi and A Malathi. Network intrusion detection using hybrid simplified swarm optimization and random forest algorithm on nsl-kdd dataset.

[10] Rainer Storn. On the usage of differential evolution for function optimization. *NAFIPS*, pages 519–523, 1996.

[11] Thanathip Sum-Im. A novel differential evolution algorithmic approach to transmission expansion planning. 2009.

[12] Xiao-Miao Zhang, Kwai Man Luk, Qing-Feng Wu, Tao Ying, Xue Bai, and Liang Pu. Cosecant-square pattern synthesis with particle swarm optimization for nonuniformly spaced linear array antennas. In *2008 8th International Symposium on Antennas, Propagation and EM Theory*, pages 193–196, 2008.

[13] Ananda Kumar Behera, Aamir Ahmad, SK Mandal, GK Mahanti, and Rowdra Ghatak. Synthesis of cosecant squared pattern in linear antenna arrays using differential evolution. In *Information & Communication Technologies (ICT), 2013 IEEE Conference on*, pages 1025–1028. IEEE, 2013.

[14] Debasis Mandal and AK Bhattacharjee. Synthesis of cosec 2 pattern of circular array antenna using genetic algorithm. In *Communications, Devices and Intelligent Systems (CODIS), 2012 International Conference on*, pages 546–548. IEEE, 2012.

[15] K.R. Subhashini, A. Baranwal, A.T. Praveen Kumar, and M.S. Reddy. Co sequent shaped pattern synthesis in spherical antenna array with excitation optimization using clever algorithms. In *India Conference (INDICON), 2014 Annual IEEE*, pages 1–6, Dec 2014.

[16] Erik De Witte, Leonidas Marantis, Kin-Fai Tong, Paul Brennan, and Hugh Griffiths. Design and development of a spherical array antenna. In *Antennas and Propagation, 2006. EuCAP 2006. First European Conference on*, pages 1–5. IEEE, 2006.

[17] L Marantis, E De Witte, and PV Brennan. Comparison of various spherical antenna array element distributions. In *Antennas and Propagation, 2009. EuCAP 2009. 3rd European Conference on*, pages 2980–2984. IEEE, 2009.

[18] Adnan Affandi[1], Mubashshir Husain, and Navin Kasim. Optimization for spherical phased array antenna.

[19] A.K. Aboul-Seoud, A.-D.S. Hafez, A.M. Hamed, and M. Abd-El-Latif. A conformal conical phased array antenna for modern radars. In *Aerospace Conference, 2014 IEEE*, pages 1–7, March 2014.

[20] Zhang Xiangjun, Ma Xiaoping, and Lai Qifeng. Two kind of conical conformal gps antenna arrays on projectile. In *Microwave, Antenna, Propagation and EMC Technologies for Wireless Communications, 2009 3rd IEEE International Symposium on*, pages 659–662, Oct 2009.

[21] N. Surendra, K.R. Subhashini, and G.L. Manohar. Cylindrical antenna array synthesis with minimum side lobe level using pso technique. In *Engineering and Systems (SCES), 2012 Students Conference on*, pages 1–6, March 2012.

[22] S. Karimkashi and Guifu Zhang. Design and manufacturing of a cylindrical polarimetric phased array radar (cppar) antenna for weather sensing applications. In *Antennas and Propagation Society International Symposium (APSURSI), 2014 IEEE*, pages 1151–1152, July 2014.

[23] Majid M Khodier and Mohammad Al-Aqeel. Linear and circular array optimization: A study using particle swarm intelligence. *Progress In Electromagnetics Research B*, 15:347–373, 2009.

Authors Biography

SATISH KUMAR REDDY M V was born to Mr. M Jagannadha Reddy and Mrs. M Thulasi on 3rd Apr, 1989 at Kadapa District, Andhra Pradesh, India. He obtained Bachelor's degree in Electronics and Communication Engineering from Narayana Engineering College , Nellore, Andhra Pradesh in 2010. He joined the Department of Electrical Engineering, National Institute of Technology, Rourkela in July 2013 as an Institute Research Scholar to pursue M.Tech degree in "Electronic Systems and Communication" specialization.